

**Best Available  
Copy  
for all Pictures**

AD-784 303

ATMOSPHERIC PRESSURE GAS LASERS

Hermann A. Haus

Massachusetts Institute of Technology

Prepared for:

Advanced Research Projects Agency  
Army Research Office

August 1974

DISTRIBUTED BY:

**NTIS**

National Technical Information Service  
U. S. DEPARTMENT OF COMMERCE  
5285 Port Royal Road, Springfield Va. 22151

AD 784303

SEMIANNUAL TECHNICAL REPORT ON  
ATMOSPHERIC PRESSURE GAS LASERS

covering the period

December 1, 1973 - May 31, 1974

submitted by

Hermann A. Haus  
Professor of Electrical Engineering

Sponsored by

Advanced Research Projects Agency  
ARPA Order No. 0675, Amend. No. 19

Contract Number: DAHC04-72-C-0044

Program Code No. :

62301E

Principal Investigator:

Hermann A. Haus  
617-253-2585

Contractor:

Massachusetts Institute of Technology  
Cambridge, Mass. 02139

Effective Date of Contract:

June 1, 1972

Short Title of Work:

Atmospheric-Pressure Gas Lasers

Expiration Date:

May 31, 1974

Date of Report:

August 1974

Amount of Contract:

\$80,000

The views and conclusions contained in this document are those of the authors, and should not be interpreted as necessarily representing the official policies, either expressed or implied, of the Advanced Research Projects Agency or the U. S. Government.

APPROVED FOR PUBLIC RELEASE; DISTRIBUTION UNLIMITED

## Introduction

The work for this research contract on atmospheric-pressure gas lasers had as its main objectives the generation of short laser pulses through mode locking and cavity dumping, the study of the nonlinear amplification processes in a transversely excited atmospheric pressure laser, and development of computer programs to check the observed amplifier responses against models of the relaxation processes of the  $\text{CO}_2$  molecule in a laser discharge.

During the progress of this work, it was realized that a simple yet reliable model of the discharge excitation of the laser medium was needed if quantitative predictions of laser performance were to be made without excessive computational effort and hence a certain loss in understanding. With this in mind an analytic model was developed for the interaction between the electrons in a molecular laser discharge with the active molecules.

One of the major bottlenecks in the generation of short laser pulses is the mode-locking process. Shorter pulses in general are obtained through the use of saturable absorber mode locking as compared with forced mode locking. The saturable absorber mode-locking process is less well understood than the forced mode-locking process. In an effort to gain a better understanding of saturable absorber mode locking a new theory of mode locking was developed. The first closed-form solution for a pulse produced by saturable absorber mode locking was obtained.

The ensuing sections of this report are addressed to one topic at a time and describe briefly the main thrust of the investigations. Details will be given in five appendices. Appendices I, II, and III contain excerpts from the Quarterly Progress Reports of the Research Laboratory of Electronics. Appendices IV and V are preprints of a paper that has been accepted for publication and of a paper that is in preparation.

### Mode Locking and Cavity Dumping

In order to produce high-intensity pulses to be used in nonlinear amplifier studies in a CO<sub>2</sub> TEA amplifier, a single pulse was selected from the laser oscillator by means of mode locking and cavity dumping. The cavity dumping scheme shuttled the mode-locked pulse out of the cavity at a time when the pulse had reached maximum intensity. In this way the full energy of the pulse inside the cavity was obtained in a single emitted pulse.

This scheme was made to work to produce single pulses 4 ns wide and with a peak power of the order of a few kilowatts. Unfortunately the power was not as high as we originally hoped because the losses of the mode-locking crystal and the electro-optic switch used for the cavity dumping were high enough to depress the laser power greatly below the value that would have been obtained without the insertion of these two elements. We then decided to select one or more pulses for the amplifier study from the mode-locked pulse train emerging

from the output mirror. In this scheme, which is described in greater detail in Appendix I, 500 kW pulses with a pulse duration of 2 ns were obtained.

#### Measurement of Short-Term Recovery of CO<sub>2</sub> Population Inversion

Sequences of pulses selected in the manner described in the preceding section were used to determine the population inversion (gain) recovery via V-V relaxation in a CO<sub>2</sub> TEA amplifying system. The amplifier was filled with a mixture of CO<sub>2</sub>, N<sub>2</sub> and helium at 200 Torr and the partial pressure of CO<sub>2</sub> was varied in the experiment from 5 Torr to 40 Torr. The individual input pulse lengths were 2 ns, the spacing between the pulses, 12 ns. The first laser pulse was made to enter the amplifier ~30  $\mu$ s after the application of the discharge current pulse. The recovery of the gain of the second pulse as a function of partial pressure of CO<sub>2</sub> was determined. The total pressure in the amplifier was sufficient for appreciable equilibration of the rotational population distribution within the duration of one pulse. Furthermore, since the rotational relaxation is mainly a function of the total pressure, and not of the partial pressure of CO<sub>2</sub>, variation of the partial pressure did not affect the recovery time of the rotational population distribution. Therefore the increased recovery as a function of increasing pressure is attributable to V-V relaxation processes. The level which has an appreciable population after equilibration of the vibrational temperatures and which

can feed the upper laser level appreciably within 12 ns at the partial pressure used is the 011 level. Hence this experiment ascertains the rate of relaxation of the 011 level and the degree of population recovery by means of this relaxation process. Figure 1 shows the result of the experiment. At the very low partial pressures when the relaxation mechanism is not operative within 12 ns the gain of the second pulse compared with that of the first one has been reduced by 20% because of the population depletion of the first pulse. The experimentally observed recovery as a function of partial pressure is shown. Two theoretical curves computed on the assumption that the recovery is due entirely to the feeding of the upper laser level by the 011 level population are shown as dashed curves. The two curves were computed for two values of population inversion changes consistent with the gain changes caused by the first pulse. This shows that the major portion of the recovery is explainable by this mechanism. The fact that the experimentally observed recovery is larger than the one predicted on the basis of the 011 level relaxation is attributable to the more effective relaxation of the lower laser level with increasing partial pressure, an effect not taken into account in the theory which assumed that even at the low partial pressures the lower laser level relaxes completely within the 12-ns interval.

Details of the experiment are given in Appendix II. The theoretical computations are contained in the Master's thesis of Y. Manichaikul.<sup>[1]</sup> The conclusion drawn from the experiment is that energy storages available in vibrational combination modes can be utilized if the pulse

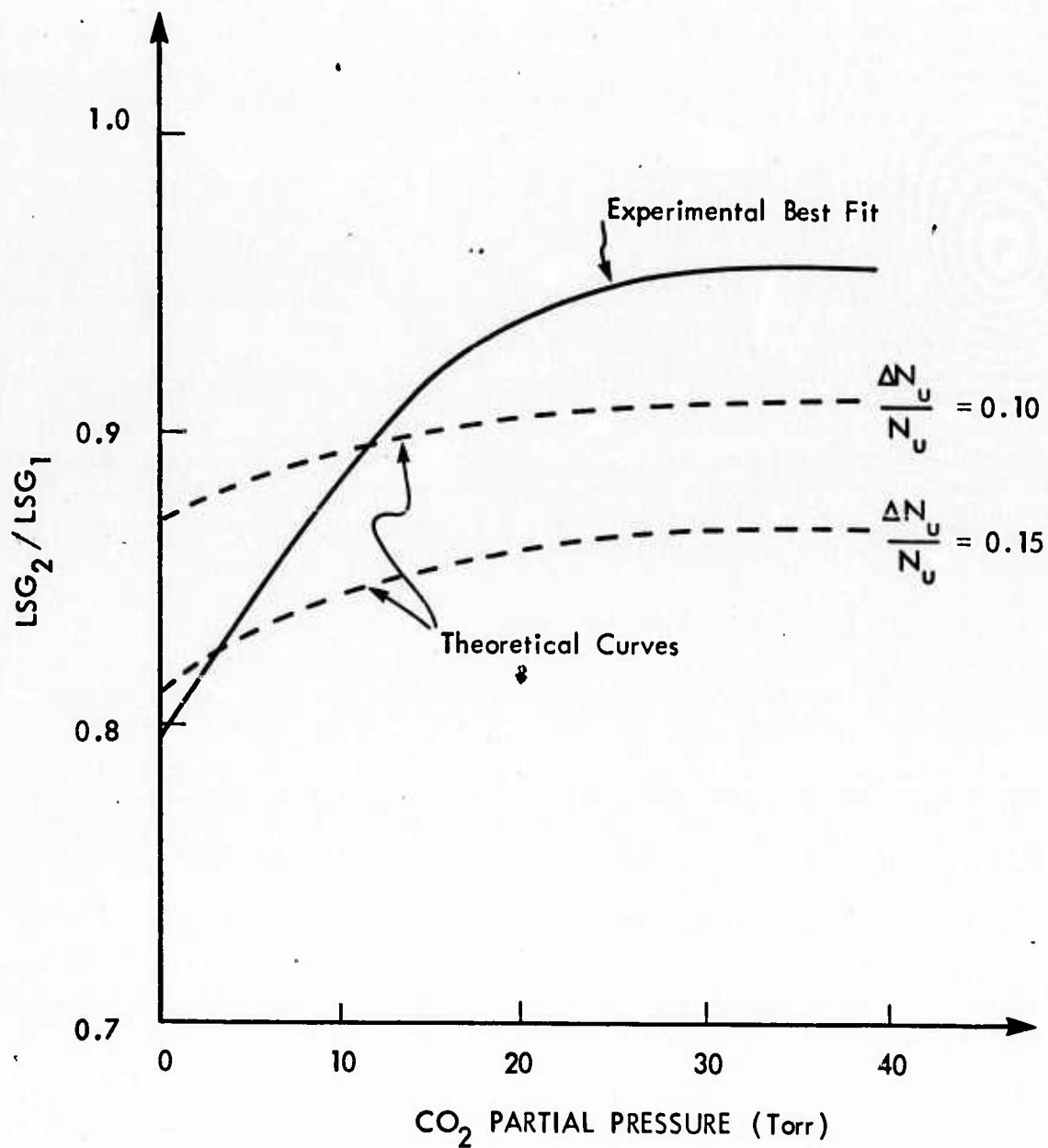


Fig. 1. Theoretical plot of LSG<sub>2</sub>/LSG<sub>1</sub> against CO<sub>2</sub> partial pressure.



to be amplified is lengthened. The present experiment indicates the magnitude of the effect and the time scales at which such utilization occurs.

#### Development of Computer Codes for Amplifier Studies

A four-temperature model including rotational relaxation for the study of pulse amplification in a TEA amplifier has been developed by A. H. M. Ross as originally proposed. The work eventually was not supported by this program but by a National Science Foundation grant. Yet Ross's results were used, for example, in the interpretation of the amplifier experiment discussed above. Ross's program is outlined in Appendix III and is available upon request.

The funds freed by the fact that NSF support was available to Ross provided the basis for two other research projects not originally proposed. These are described below.

Electron Distribution and Lasing Efficiency. Computer codes evaluating the electron distribution and the pumping of laser levels have been developed in several laboratories, notably at United Aircraft Corporation. Whereas good quantitative results can be obtained from these programs, it is difficult to cull from them physical insight about the influence of various parameters, without carrying out costly computations. With this in mind, we have developed a simplified model for the electron distribution and the pumping of the electron

laser levels which is amenable to closed-form solutions. The details of this work have been published.<sup>[2]</sup> Here we give a brief summary of the salient features.

By simplifying the energy dependence of the collision cross sections of the electrons, it was possible to obtain a closed-form solution for the electron distribution, a function of the degree of molecular excitation. In this way the feedback could be ascertained of the changes in the molecular population inversion upon the electron distribution. Also the question could be asked to what extent the i-v characteristic of a preionized laser (E-beam laser) depends upon the lasing action. It was found that the i-v characteristic depends only weakly upon lasing; in fact when the elastic collision frequency of the electrons is assumed independent of electron energy, the i-v characteristic is entirely independent of whether lasing does or does not occur. The energy extraction by induced emission is offset by a decrease of the energy transfer to the translational modes of the gas. For other details we refer to the publication itself.

### Mode-Locking Theory

A major bottleneck in the production of short laser pulses is the mode-locked oscillator. Extensive work has been done on the theory of mode locking, but no simple analysis has been published on the theory of mode locking by a saturable absorber. In an effort to develop a closed-form theory for saturable absorber mode locking, we arrived

at a greatly simplified theory of forced mode locking which enabled us to solve hitherto unsolved problems. A paper has been submitted to the Journal of Quantum Electronics and revised upon request of the reviewers. The revised version is attached as Appendix IV. The new problems that have been solved are (a) forced mode locking of an inhomogeneously broadened laser medium, (b) forced mode locking by square-wave amplitude modulation, and (c) stability analysis of the forced mode-locked pulse train.

A closed-form solution has been obtained for the mode-locked pulse of a homogeneously broadened laser mode locked by a saturable absorber of relaxation time that is short compared with the pulse length. Details are given in a preprint which forms Appendix V.

#### References

1. Yongyut Manichaikul, "Generation and Amplification of High-Intensity Nanosecond TEA CO<sub>2</sub> Laser Pulses," S. M. Thesis, Department of Electrical Engineering, M. I. T., September 1973.
2. W. P. Allis and H. A. Haus, "Electron Distributions in Gas Lasers," J. Appl. Phys. 45, 781-791 (February 1974).

APPENDIX I

Reprinted from

Quarterly Progress Report No. 110, July 15, 1973

Research Laboratory of Electronics  
Massachusetts Institute of Technology  
Cambridge, Massachusetts 02139

## VI. APPLIED PLASMA RESEARCH

## D. Laser-Plasma Interactions

Academic and Research Staff

Prof. E. V. George  
Prof. A. Bers

Prof. H. A. Haus  
Dr. A. H. M. Ross

J. J. McCarthy  
W. J. Mulligan

Graduate Students

Y. Manichaikul  
J. L. Miller

D. Prosnitz

C. W. Werner  
D. Wildman

### 1. GENERATION AND AMPLIFICATION OF HIGH-INTENSITY, NANOSECOND TEA CO<sub>2</sub> LASER PULSES

National Science Foundation (Grant GK-33843)

U. S. Army - Research Office - Durham (Contract DAHC04-72-C-0044)

Y. Manichaikul

We have reported previously on generation of short nanosecond pulses from a pin resistor TEA CO<sub>2</sub> laser by way of mode locking and cavity dumping.<sup>1</sup> Single pulses 4 ns wide (full width at half maximum, FWHM) with peak power ~1 kW were produced. Problems were encountered with the system and a new one was built. The problems, and the changes that have been made in the new system, are as follows.

(i) The peak power obtained from the previous system was too low for some experiments. For example, to saturate a TEA CO<sub>2</sub> laser amplifier requires a peak power of intensity greater than 100 kW/cm<sup>2</sup>. In our new system we use a 3-electrode TEA CO<sub>2</sub> discharge tube which has a higher gain than the pin-resistor TEA CO<sub>2</sub> discharge tube.<sup>2</sup> With this improved system we have obtained mode-locked pulses of peak powers in excess of 500 kW.

(ii) A germanium acousto-optic modulator at Brewster angle is now being used. This eliminates the power-density limitation that arose in the old system, which used an antireflection-coated germanium modulator.

(iii) An antireflection-coated GaAs crystal is now placed outside, rather than inside, the optical cavity, which makes alignment of the cavity less critical. Also, since the antireflection coating of the GaAs crystal was slightly damaged, there is less distortion of the TEM mode when the crystal is outside the cavity.

(iv) In the old system the high-voltage supply to the cavity-dumping GaAs crystal was falsely triggered by electrical noise generated by the laser discharge tube. In the new system a laser-induced spark gap<sup>3</sup> is used to eliminate this problem.

(v) Previously, continuous RF power was supplied to the germanium mode-locking



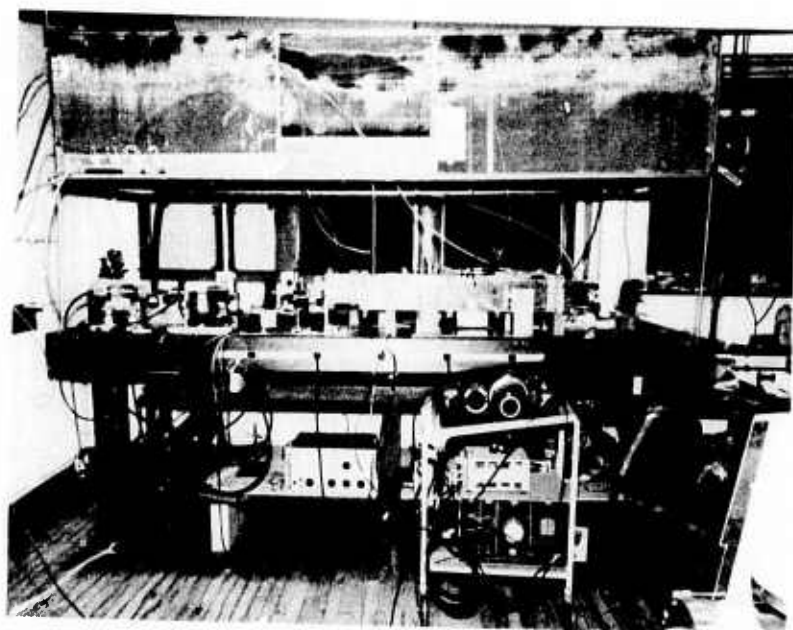
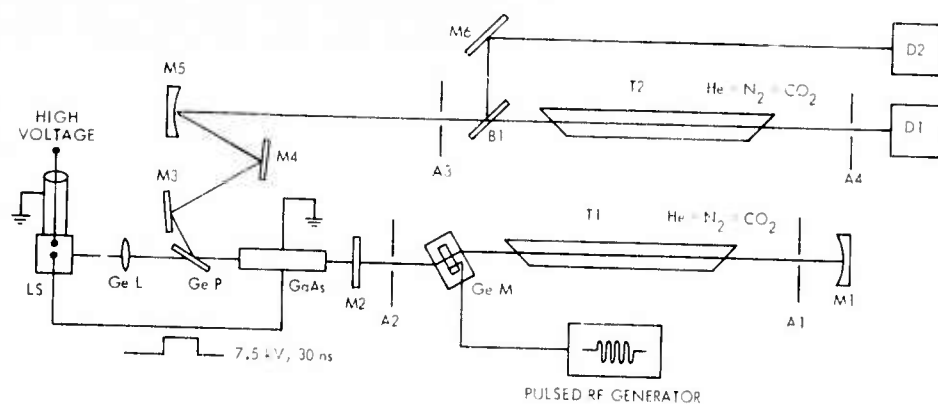


Fig. VI-22.  
Photograph of experimental  
apparatus.



- |                |  |
|----------------|--|
| A1, A2, A3, A4 | Apertures  |
| B1             | NaCl beam splitter   |
| D1             | Gold-doped detector  |
| D2             | Copper-doped detector  |
| GaAs           | Electro-optic modulator  |
| Ge L           | Germanium lens, 1.5" focal length                              |
| Ge M           | Germanium acousto-optic modulator                              |
| Ge P           | Germanium plate at Brewster angle                              |
| LS             | Laser-induced spark gap  |
| M1             | Gold-coated mirror, 99.6 % reflecting, 4 m radius of curvature |
| M2             | Germanium mirror, 20 % transmitting                            |
| M3, M4, M6     | Gold-coated flat mirrors, totally reflecting                   |
| M5             | Gold-coated mirror, 99.6 % reflecting, 2 m radius of curvature |
| T1, T2         | 3-electrode discharge tubes, 1 m long                          |

Fig. VI-23. Diagram of experimental arrangement.

## (VI. APPLIED PLASMA RESEARCH)

crystal. This caused the germanium crystal to heat up, thereby changing its acoustic resonance frequencies. We are now using pulsed RF power to minimize this problem.

#### Experimental Arrangement

Figure VI-22 is a photograph of the new ns TEA  $\text{CO}_2$  laser pulse-producing system, and Fig. VI-23 is a schematic diagram of the experimental arrangement. With a dc voltage of 5 kV across the GaAs electro-optic modulator a fraction of the energy from the beam can be switched out at the Brewster-angle germanium plate (GeP, see Fig. VI-23). This fraction of the beam was guided by two flat mirrors to a gold-coated mirror with 2-m radius of curvature, which focuses the beam inside the 3-electrode laser amplifier. The tube is operated between 10 Torr and 400 Torr. A fraction of the beam, before going into the amplifier, is reflected out from a beam splitter and detected by a copper-doped liquid-helium-cooled detector with a rise time of  $<1$  ns. The fraction of the beam that has passed through the amplifier is detected by a gold-doped liquid-nitrogen-cooled detector with a rise time of  $\sim 1$  ns.

#### Experiments

##### a. Generation of Nanosecond TEA $\text{CO}_2$ Laser Pulses

The laser cavity has an optical length of approximately 1.88 m. To achieve forced mode locking, RF driving power at 2.5 ms with 4 W peak power was supplied to the germanium acousto-optic modulator. The 3-electrode discharge tube inside the cavity is set to trigger at 2 ms after the RF power is on. We have obtained mode-locked pulses  $< 2$  ns wide (FWHM) with a peak power of  $\sim 500$  kW. Figure VI-24 shows a typical train of mode-locked pulses detected by a copper-doped detector and displayed on a Tektronix 7904 oscilloscope.

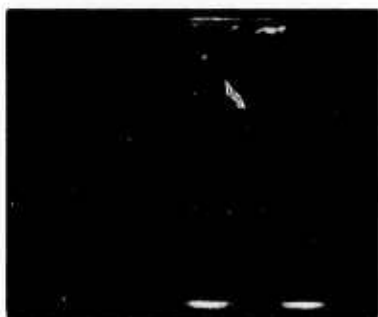


Fig. VI-24.

Typical mode-locked pulses from the laser oscillator (5 ns/div).

The switching out of individual pulses is accomplished by using the laser-induced spark gap, which is normally filled with prepurified nitrogen at 100 psi. The coaxial cable was charged up to 15 kV. We can vary the temporal triggering of this gap by

## (VI. APPLIED PLASMA RESEARCH)

altering the nitrogen pressure, the distance between the two electrodes of the spark gap, or both. When the spark gap is triggered, a square voltage pulse of 7.5 kV, twice the length of cable, is produced. This pulse is supplied to the GaAs crystal, which rotates the polarization of the desired number of mode-locked pulses. These mode-locked pulses are then reflected out of the train at the Brewster-angle germanium plate.

b. Amplification of Nanosecond TEA  $\text{CO}_2$  Laser Pulses

Three pulses from a train of mode-locked pulses were switched out and guided through an amplifier tube. These pulses were measured before and after they propagated through the laser amplifier. Figure VI-25 shows input and output signals detected by

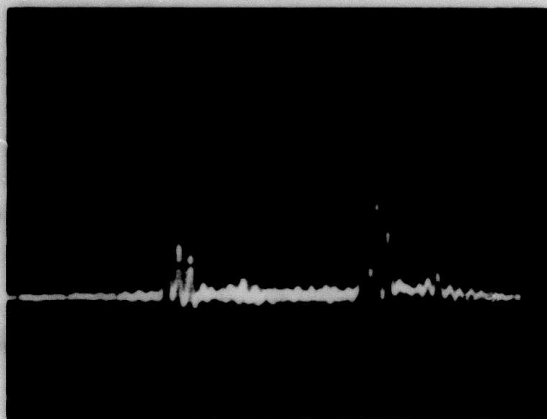


Fig. VI-25.

Input and output pulse trains of the laser amplifier. An artificial 200-ns electrical delay facilitated the display (50 ns/div).

copper-doped and gold-doped germanium detectors, respectively. The output signal from the gold-doped germanium detector was artificially delayed 200 ns by use of a coaxial delay line. By using the add-mode on a Tektronix 454A oscilloscope, we were able to display both signals on a single trace.

In our preliminary studies we have found that the first pulse of our three laser pulses is of sufficient power density to saturate the laser amplifier. Further work on this aspect of the experiment will be described in a future report.

#### References

1. Y. Marichaikul and E. E. Stark, Jr., Quarterly Progress Report No. 107, Research Laboratory of Electronics, M.I.T., October 15, 1972, pp. 81-84.
2. P. R. Pearson and H. M. Lamberton, "Atmospheric Pressure  $\text{CO}_2$  Lasers Giving High Output Energy Per Unit Volume," IEEE J. Quant. Electronics, Vol. QE-8, No. 2, pp. 145-149, February 1972.
3. A. V. Nurmikko, IEEE J. Quant. Electronics, Vol. QE-7, No. 9, pp. 470-471, September 1971.



A 14

## APPENDIX II

Reprinted from

Quarterly Progress Report No. 111, October 15, 1973

Research Laboratory of Electronics  
Massachusetts Institute of Technology  
Cambridge, Massachusetts 02139

## 2. AMPLIFICATION OF TWO HIGH-INTENSITY NANOSECOND TEA CO<sub>2</sub> LASER PULSES (AHN)

National Science Foundation (Grant GK-37979X)

U. S. Army - Research Office - Durham (Contract DAHC04-72-C-0044)

Y. Manichaikul

### Experiment

We have previously reported on the generation and amplification of high-intensity nanosecond pulses.<sup>1</sup> Two or three of these pulses were produced. They were from the P(16) transition, 2 ns wide (FWHM), separated by 12 ns. When these pulses were focused into a three-electrode laser amplifier as shown in Fig. VI-12, a peak intensity of 2-3 MW/cm<sup>2</sup> was obtained. A beam splitter was used so that the intensity of the pulses could be monitored. The input and output detectors were as shown in Fig. VI-12. In this experiment the detected input signals were delayed 100 ns by using 60 ft of

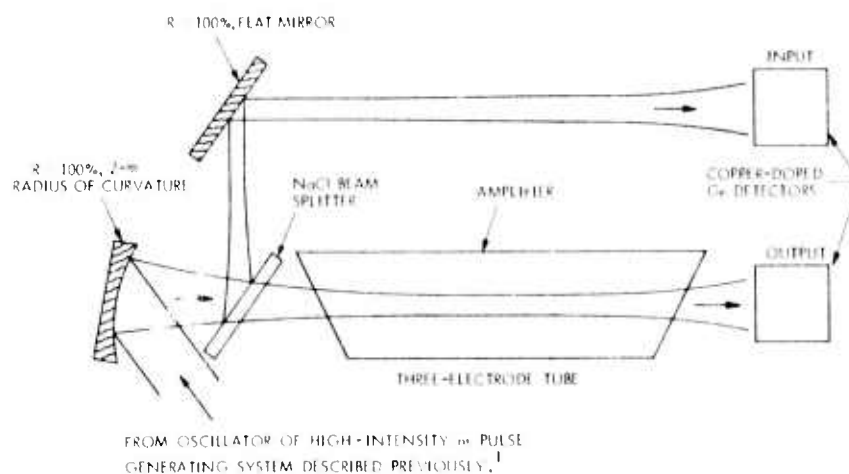


Fig. VI-12. Experimental arrangement for amplification of high-intensity ns pulses. (See Y. Manichaikul.<sup>1</sup>)

RG-8 cable. The add mode of a Tektronix oscilloscope was used to display the signals for both input and output pulses on the same screen. The two detectors were calibrated against each other by comparing the oscilloscope picture of the input and output pulses without discharge exciting the three-electrode laser amplifier. Figure VI-13a shows

## (VI. APPLIED PLASMA RESEARCH)

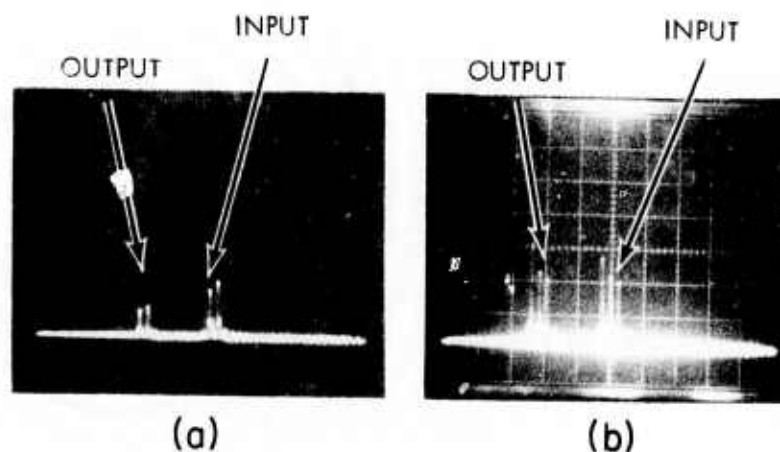


Fig. VI-13. Output and input of AHN experiment. Total pressure: 200 Torr. Gas mixture:  $\text{CO}_2:\text{N}_2:\text{He} = \text{X}:4:100$ . Intensity of input pulse:  $0.75 \text{ (MW/cm}^2\text{)/div}$ . Intensity of output pulse:  $1.12 \text{ (MW/cm}^2\text{)/div}$ . Time:  $50 \text{ ns/div}$ . (a) Amplifier off. (b) Amplifier on.

the oscilloscope display for this case.

In order to probe the temporal evolution of the three-electrode laser amplifier, we first fired the amplifier and, after a chosen delay time, the oscillator. In general, the oscillator was fired  $\sim 30 \mu\text{s}$  after the onset of the discharge in the amplifier for two reasons: first, we wished to avoid the effects on our measurements of the shock waves generated by the discharge. Second, we wished to be certain that the symmetric stretching (SS) and bending (B) modes of  $\text{CO}_2$  had equilibrated with each other at slightly above the kinetic temperature of the gas.<sup>2</sup>

Measurements on the amplification of high-intensity ns pulses were made at 200 Torr of  $\text{CO}_2:\text{N}_2:\text{He}$  mixtures. The ratio of these mixtures was  $\text{CO}_2:\text{N}_2:\text{He} = \text{X}:4:100$ , where  $\text{CO}_2$  partial pressure was varied from 3.5 to 35 Torr partial pressure. Small-signal gain of this three-electrode laser amplifier in each case was measured by a cw  $\text{CO}_2$  laser.

### Results

Figure VI-13b illustrates the input and output pulses when the amplifier is turned on. Four such measurements were made and their average was taken at each  $\text{CO}_2$  partial pressure studied. We have found that the RG-8 cable used for the time delay introduces some distortion in the input signals. This distortion can be accounted for if the first (second) pulses of the input and output pulses from the amplification measurements are compared with the first (second) pulses of the input and output pulses when the amplifier was evacuated.

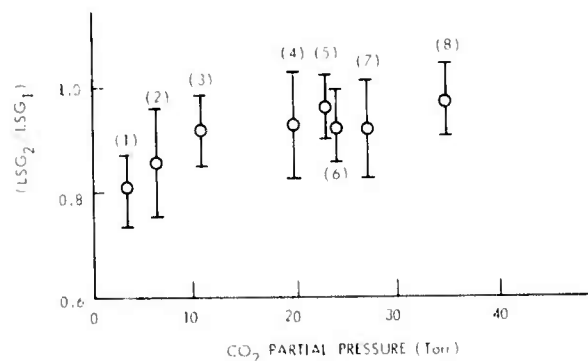


Fig. VI-14.  $LSG_2/LSG_1$  vs partial  $CO_2$  pressure.

Table VI-1. Experimental results.

No.	$P_{CO_2}$ (Torr)	SSG $\pm 10\%$	$LSG_1$ $\pm 10\%$	$T_{vv}^a$ (°K)	$\frac{\Delta N_u}{N_u(0)}$
1	3.5	0.50	0.30	1180	0.12
2	6.5	0.70	0.36	1150	0.11
3	11.0	1.50	0.76	1155	0.14
4	20.0	1.00*	0.52	845	0.11
5	23.0	1.50*	0.75	860	0.13
6	24.0	2.00*	0.96	890	0.14
7	27.0	2.50*	1.15	935	0.15
8	35.0	2.00	0.81	830	0.10

Notes: \* Not measured directly; calculated from  $LSG_1$  and the peak intensity of the pulse.

$SSG = \frac{I_{in} - I_{out}}{I_{in}}$  is the small-signal gain across the tube.

Here the intensity is less than  $1 \text{ W/cm}^2$ .

$LSG_1$ , large-signal gain of the first pulse.

$T_{vv}^a$ , temperature of the asymmetric stretching mode calculated from SSG.

$\frac{\Delta N_u}{N_u(0)}$ , fractional depletion of the  $00^0 1$  population by an  $N_u(0)$  ns pulse.

$\Delta N_u$ , calculated from the large-signal gain and the intensity of the pulse.

$N_u(0)$ , obtained from SSG.

A 18

(VI. APPLIED PLASMA RESEARCH).

Figure VI-14 shows  $LSG_2/LSG_1$  vs the partial pressure of  $CO_2$  studied. We have

$$LSG_i = \frac{\Delta I_{out i} - I_{ini}}{I_{ini}},$$

where  $i = 1, 2$ , with 1 and 2 representing first and second pulses.  $LSG_1$  ( $LSG_2$ ) is the large-signal gain of the first (second) pulses. The following observations can be made from these measurements. (i)  $LSG_2/LSG_1$  is less than unity. This is to be expected, since the first pulse had depleted a fraction of the population from the  $00^{\circ}1$  level of  $CO_2$ . (ii) The ratio  $LSG_2/LSG_1$  is approximately 0.8 at  $CO_2$  partial pressure of 3.5 Torr and the ratio increases slowly to 0.9 as  $CO_2$  partial pressure increases to 20 Torr or higher, which is as expected, since the  $00^{\circ}1$  level of  $CO_2$  was being repopulated by the higher  $O n^{\ell} m$  levels at a rate<sup>3</sup> that is directly proportional to the  $CO_2$  partial pressure.

Table VI-1 gives other experimental results of interest. We found that the large-signal gain of our pulses is approximately one-half the small-signal gain, and the fractional depletion of the  $00^{\circ}1$  level,  $\frac{\Delta N_u}{N_u(0)}$ , is between 0.10 and 0.15.

A theoretical model for the amplification of high-intensity nanosecond pulses is being developed. We shall present the theory, and make a comparison of theory and experiment in a future report.

#### References

1. Y. Manichaikul, "Generation and Amplification of High-Intensity, Nanosecond TEA  $CO_2$  Laser Pulses," Quarterly Progress Report No. 110, Research Laboratory of Electronics, M. I. T., July 15, 1973, pp. 118-121.
2. D. L. Lyon, IEEE J. Quant. Electronics, Vol. QE-9, No. 1, pp. 139-153, January 1973.
3. I. Burak, Y. Noter, and A. Szöke, IEEE J. Quant. Electronics, Vol. QE-9, No. 5, pp. 541-544, May 1973.

A-19

APPENDIX III

Reprinted from

Quarterly Progress Report No. 111, October 15, 1973

Research Laboratory of Electronics  
Massachusetts Institute of Technology  
Cambridge, Massachusetts 02139

## VI. APPLIED PLASMA RESEARCH

## D. Laser-Plasma Interactions

Academic and Research Staff

Prof. E. V. George  
Prof. A. Bers

Prof. H. A. Haus  
Dr. A. H. M. Ross

J. J. McCarthy  
W. J. Mulligan

Graduate Students

Y. Manichaikul  
J. L. Miller

D. Prosnitz

C. W. Werner  
D. Wildman

1. CO<sub>2</sub> SHORT-PULSE AMPLIFICATION STUDIES

National Science Foundation (Grant GK-37979X)

A. H. M. Ross

Recent advances in high-pressure gas discharge technology have made possible the deposition of as much as 300 joules/liter in carbon dioxide laser media. Because of the several vibration-rotation degrees of freedom of the CO<sub>2</sub> molecule, this energy is stored in a great many molecular states, and therefore efficient extraction of it requires optical pulse lengths that are large compared with the kinetic collision times governing the energy-exchange processes in the medium. Operation of high-pressure devices as oscillators yields as much as 50 joules/liter from the afterglow of a pulsed discharge, and quasi cw operation has given hundreds of joules/liter in 10-100  $\mu$ s pulses. Extraction in ns pulses is far less efficient. In this report we summarize theoretical results from a multitemperature kinetic model formulated to describe ns pulse amplification by devices operating at pressures above 1 atm. Numerical results for 1-atm and 5-atm pulse amplifiers are presented.

Amplification of pulses comparable to, or faster than, kinetic collision times requires consideration of the polarization of the molecules, and of inertial effects in the molecular dipoles (for example, see Hopf and Rhodes<sup>1</sup>). Theoretical models incorporating only two vibration states and the full rotation spectrum will be adequate descriptions. If energy is to be extracted efficiently, the pulse length must be several collision times, in which case the coherence effects can be neglected, and the medium can be described by a rate-equation model.

In the rate-equation limit the growth of a plane wave in a transversely uniform medium with nonresonant loss  $\sigma$  can be described by a first-order differential equation in distance

$$\left(\frac{\partial I}{\partial z}\right)_t = -\alpha I + \sigma(\omega) N_c \left\{ [00^0 1, J'] - \frac{g_{J'}}{g_J} [10^0 0, J] \right\} I, \quad (1)$$

## (VI. APPLIED PLASMA RESEARCH)

where the stimulated emission cross section is

$$\sigma(\omega) = \frac{\lambda^2}{4\pi t_{sp}} \frac{\gamma_{JJ'}^2}{g_{J'}} \frac{\gamma_0}{(\omega - \omega_0)^2 + \gamma_0^2}, \quad (2)$$

with  $N_c$  the  $\text{CO}_2$  density,  $g_J$  the degeneracy of the  $J^{\text{th}}$  rotational state

$$g_J = 2J + 1, \quad (3)$$

and  $[n_1 n_2 n_3, J]$  is the fractional  $\text{CO}_2$  population in the state of these quantum numbers (that is, the diagonal element of the density matrix for a single molecule). The spontaneous emission time written here is that for the entire band; an individual line has a matrix element proportional to the rotational matrix element

$$\gamma_{JJ'}^2 = \begin{cases} J & \text{for a P(J) line } (J' = J - 1) \\ J + 1 & \text{for an R(J) line } (J' = J + 1) \end{cases} \quad (4)$$

We shall neglect frequency pulling effects, although in high-gain systems they will be important if the input pulse is detuned appreciably.

We assume that the molecular kinetics can be described adequately by rate equations in which only binary collisions are important. Even with the rate-equation model, the six degrees of freedom of the  $\text{CO}_2$  molecule in its electronic ground state give rise to so many important vibration-rotation states that the problem would be intractable without further simplifying assumptions. The fact that the molecule is reasonably harmonic in its low vibrational states, and that the interaction of vibration and rotation is weak allows us to treat the relaxation of the various degrees of freedom substantially independently. We also make use of the observation of Osipov and Stupochenko<sup>2</sup> that relaxation of molecular vibrations from a nonequilibrium distribution takes place in two phases: first, a rapid relaxation to quasi equilibrium in which the various normal modes of the molecule acquire a Boltzmann distribution of excitation, which can correspond to a temperature far different from the kinetic temperature of the gas and second, a slow relaxation of these quasi-equilibrium distributions to the kinetic temperature.

Since we are concerned with amplifiers in which the pumping takes place over a time scale that is large compared with the kinetic collision times, it is reasonable to assume that prior to the arrival of the electromagnetic pulse the vibrational states are distributed according to the partial equilibrium distribution

$$[n_1 n_2 n_3] = (1-s)(1-b)^2 (1-a) s^{n_1} (n_2+1) b^{n_2} a^{n_3}, \quad (5)$$



(VI. APPLIED PLASMA RESEARCH)

where  $s$ ,  $b$ , and  $a$  are Boltzmann factors for the symmetric stretch, bending, and asymmetric stretch modes ( $v_1, v_2, v_3$ ) of the  $\text{CO}_2$  molecule. We have taken the state  $[n_1 n_2 n_3]$  to include all of the states  $[n_1 n_2^\ell n_3]$ , of which there are  $n_2 + 1$  ( $\ell$  represents an angular momentum around the symmetry axis of the molecule, and hence can take on the values  $-n_2, -n_2 + 2, -n_2 + 4, \dots, n_2 - 2, n_2$ ).

$$s = \exp \left[ - \frac{\epsilon_s}{k_B T_s} \right] \quad (6)$$

$$b = \exp \left[ - \frac{\epsilon_b}{k_B T_b} \right] \quad (7)$$

$$a = \exp \left[ - \frac{\epsilon_a}{k_B T_a} \right]. \quad (8)$$

The rotation states also reflect a Boltzmann distribution

$$[n_1 n_2^\ell n_3, J] = [n_1 n_2^\ell n_3]^2 g_J \left( \frac{hcB}{k_B T_r} \right) \exp \left[ - \frac{hcB}{k_B T_r} J(J+1) \right], \quad (9)$$

where we assume that the rotational constant  $B$  is independent of the vibrational state ( $\text{CO}_2$  has  $cB = 11606$  MHz and  $11698$  MHz in the upper and lower laser levels, respectively). Doppler broadening of the laser lines is less than 1% of the homogeneous linewidth at 1 atm, so the velocity distribution of the molecules will be neglected.

Passage of an optical pulse will introduce deviations from these distributions. In particular, a fast pulse will create a "hole" in the state  $[00^\circ 1, J']$  (that is, it will depress the population below that given by (5)), and a "peak" in  $[10^\circ 0, J]$  because of the stimulated emission process. Judicious approximations allow a description of the kinetics in terms of variables giving the average occupations of the three vibrational modes and the depths of the "holes" in both vibration and rotation. In particular, we assume that the two laser states have the forms

$$[00^\circ 1] = z_v^{-1} a + \alpha \quad (10)$$

$$[10^\circ 0] = Z_v^{-1} s + \beta \quad (11)$$

and that the other states retain their previous occupation probability exclusive of normalization

$$[n_1 n_2 n_3] = Z_v^{-1} s^{n_1} (n_2 + 1) b^{n_2} a^{n_3}, \quad (n_1 n_2 n_3) \neq \text{laser state}. \quad (12)$$

## (VI. APPLIED PLASMA RESEARCH)

The normalization condition requires

$$Z_v^{-1} = (1-a-\beta)(1-s)(1-b)^2 (1-a). \quad (13)$$

Defining the occupation fractions for the individual modes

$$x_q = \sum_{mn} [mnq] \quad (14)$$

$$y_n = \sum_{mq} [mnq] \quad (15)$$

$$z_m = \sum_{nq} [mnq], \quad (16)$$

and with the assumptions (10), (11), and (12), we find the following expressions.

$$\left. \begin{aligned} x_q &= (1-a-\beta)(1-a)a^q, & q \neq 0 \text{ or } 1 \\ x_0 &= 1 - a - a + (a+\beta)a = (1-a-\beta)(1-a) + \beta \\ x_1 &= (1-a-\beta)(1-a)a + a \end{aligned} \right\} \quad (17)$$

$$y_n = (1-a-\beta)(n+1)b^n \quad (18)$$

$$\left. \begin{aligned} z_m &= (1-a-\beta)(1-s)s^m, & m \neq 0 \text{ or } 1 \\ z_0 &= 1 - s - \beta + (a+\beta)s = (1-a-\beta)(1-s) + a \\ z_1 &= (1-a-\beta)(1-s)s + \beta. \end{aligned} \right\} \quad (19)$$

These distributions are illustrated in Fig. VI-8.

While this assumption of "holes" in single vibrational states is a convenient approximation, the corresponding ansatz for the rotational distribution is supported experimentally by the work of Cheo and Abrams.<sup>3</sup> They have found that the rotational relaxation may be J-independent and all rotational levels are thermalized in one collision time, so that the expression

$$[00^{\circ} 1, J'] = [00^{\circ} 1] \left\{ Z_r^{-1} 2 g_{J'} \exp \left[ - \left( \frac{hcB}{k_B T_r} \right) J'(J'+1) \right] + \xi \right\} \quad (20)$$

with

## (VI. APPLIED PLASMA RESEARCH)

$$Z_r^{-1} = (1-\xi) \left( \frac{hcB}{k_B T_r} \right) \quad (21)$$

correctly parametrizes solutions of the model.  $\xi$  measures the depth of the "hole" in the rotational sublevel depleted by the radiation; the other levels are populated

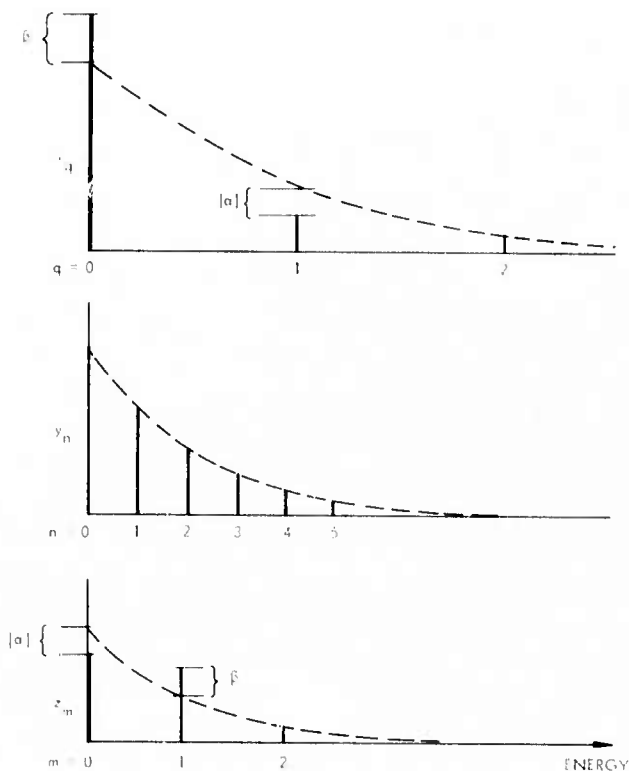


Fig. VI-8. Assumed distributions of  $\text{CO}_2$  normal vibrational mode excitations.

in proportion to a Boltzmann distribution scaled in amplitude by  $1-\xi$  so that the net vibrational-state population is held constant as  $\xi$  varies. A similar expression is assumed for the lower level:

$$[10^0 0, J] = [10^0 0] \left\{ Z_r^{-1} 2 g_J \exp \left[ - \left( \frac{hcB}{k_B T_r} \right) J(J+1) + \eta \right] \right\} \quad (22)$$

with

$$Z_r^{-1} = (1-\eta) \left( \frac{hcB}{k_B T_r} \right). \quad (23)$$

This rotational distribution is illustrated in Fig. VI-9.

## (VI. APPLIED PLASMA RESEARCH)

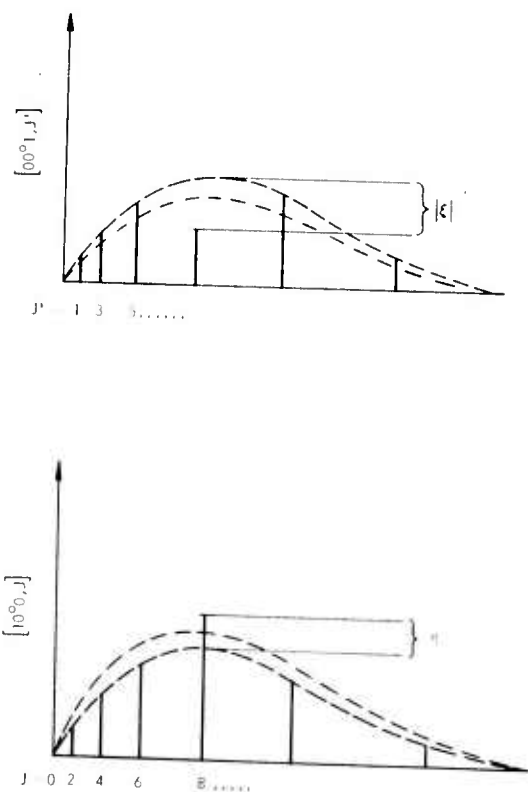
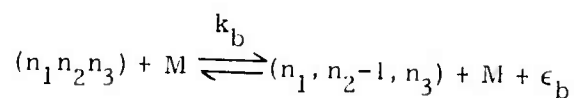


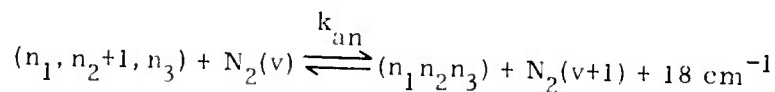
Fig. VI-9. Assumed distributions of  $\text{CO}_2$  rotational-state excitations.

The Landau-Teller assumption<sup>4</sup> that the dependence of energy exchange cross sections is that of harmonic oscillator matrix elements can be used to determine the cross sections for the processes to all orders from the measured rates. We have taken into account the following processes.

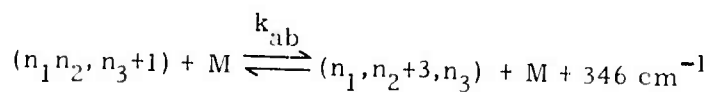
V-T in the  $\nu_2$  mode:



Intermode V-V between  $\nu_3$  and  $\nu_N$ :

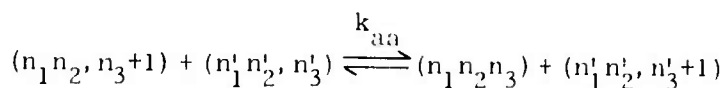


Intermode V-V between  $\nu_3$  and  $3\nu_2$ :

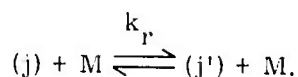


## (VI. APPLIED PLASMA RESEARCH)

Intramode V-V in  $v_3$ :



R-T:



In addition, the lower laser state has been assumed to have a V-V relaxation of indeterminate nature which has been modeled by a simple exponential decay. Other V-T processes could be included, but the principal loss rate from both  $v_3$  and  $v_N$  is by the  $v_2$  mode. Also, because of the close coupling of the  $v_1$  and  $v_2$  modes by the Fermi resonance (that is, large cross sections for the conversion of one member of a Fermi resonant pair into the other), we have assumed that the  $v_1$  and  $v_2$  vibrational temperatures are equal. The proper variable for the description of the combined bath of states is

$$Q = 2S + B, \quad (24)$$

where S and B are the average occupancies of  $v_1$  and  $v_2$ :

$$S = \sum_m m z_m = Z_v^{-1} \frac{s}{1-s} + \beta, \quad (25)$$

$$B = \sum_n n y_n = Z_v^{-1} \frac{2b}{1-b}, \quad (26)$$

$$A = \sum_q q x_q = Z_v^{-1} \frac{a}{1-a} + \alpha. \quad (27)$$

For simplicity, we have also assumed  $\epsilon_s = 2\epsilon_b$  so that

$$s = b^2. \quad (28)$$

The derivation of the equations for A, N, Q,  $\alpha$ ,  $\beta$ ,  $\xi$ ,  $\eta$  and the kinetic-rotational energy per particle is straightforward but tedious. Neglecting the  $\alpha + \beta$  terms in (17)-(19) compared to 1, we find ( $\omega = \omega_0$ ):

$$\begin{aligned} \frac{\partial A}{\partial t} = & -R_{an} \left[ A(N+1) - (A+1)N e^{-\epsilon_{an}/k_B T} \right] \\ & -R_{ab} \left[ 1 + \frac{3B}{B+2} \right] \left[ A \left( \frac{B}{2} + 1 \right)^3 - (A+1) \left( \frac{B}{2} \right)^3 e^{-\epsilon_{ab}/k_B T} \right] \\ & -R_i \end{aligned} \quad (29)$$

## (VI. APPLIED PLASMA RESEARCH)

$$\begin{aligned} \frac{\partial Q}{\partial t'} = & +3R_{ab} \left[ 1 + \frac{3B}{B+2} \right] \left[ A \left( \frac{B}{2} + 1 \right)^3 - (A+1) \left( \frac{B}{2} \right)^3 e^{-\epsilon_{ab}/k_B T} \right] \\ & - R_b \left( \frac{B - \bar{B}}{\frac{B}{2} + 1} \right) + 2R_i \end{aligned} \quad (30)$$

$$\frac{\partial N}{\partial t'} = R_{na} \left[ A(N+1) - (A+1)N e^{-\epsilon_{an}/k_B T} \right] \quad (31)$$

$$\frac{\partial a}{\partial t'} \approx -2R_{aa} a - R_i \quad (32)$$

$$\frac{\partial \beta}{\partial t'} \approx -2R_{bb} \beta + R_i \quad (33)$$

$$\frac{\partial \xi}{\partial t'} = -\gamma_r \xi - (1-\xi) R_i / [00^\circ 1] \quad (34)$$

$$\frac{\partial \eta}{\partial t'} = -\gamma_r \eta + (1-\eta) R_i / [10^\circ 0] \quad (35)$$

$$\begin{aligned} \left( \frac{3}{2} + \psi_c + \psi_n \right) \frac{\partial}{\partial t'} (k_B T) = & \psi_c \epsilon_b R_b \left( \frac{B - \bar{B}}{\frac{B}{2} + 1} \right) \\ & + \psi_c \epsilon_{an} R_{an} \left[ A(N+1) - (A+1)N e^{-\epsilon_{an}/k_B T} \right] \\ & + \psi_c \epsilon_{ab} R_{ab} \left( 1 + \frac{3B}{B+2} \right) \left[ A \left( \frac{B}{2} + 1 \right)^3 - (A+1) \left( \frac{B}{2} \right)^3 e^{-\epsilon_{ab}/k_B T} \right], \end{aligned} \quad (36)$$

where

$$\psi_c R_{an} = \psi_n R_{na} = \psi_c \psi_n k_{an} P \quad (37)$$

$$R_{ab} = \sum_M \psi_M k_{ab}^{(M)} P \quad (38)$$

$$R_b = \sum_M \psi_M k_b^{(M)} P \quad (39)$$

$$R_{aa} = \psi_c k_{aa} P \quad (40)$$

$$\bar{B} = B(T_b = T) \quad (41)$$

## (VI. APPLIED PLASMA RESEARCH)

$$R_1 = \sigma(\omega_0) \left\{ [00^\circ 1, J'] - \frac{g_{J'}}{g_J} [10^\circ 0, J] \right\} \frac{I}{h\nu}. \quad (42)$$

Equations 1 and 29-36 (which are in the canonical form of a set of hyperbolic equations if  $t'$  is the retarded time  $t - z/c$ ) have been solved numerically for a 30%  $\text{CO}_2$  gas mixture at 1 atm and 5 atm total pressure. The input pulse was a 1 ns (FWHM),  $1 \text{ MW/cm}^2$  Gaussian shape. Initial conditions were calculated under the assumption of equilibration of  $Q$  at  $T_0$ , and of  $T_a = T_n$  sufficient to give the small-signal gains

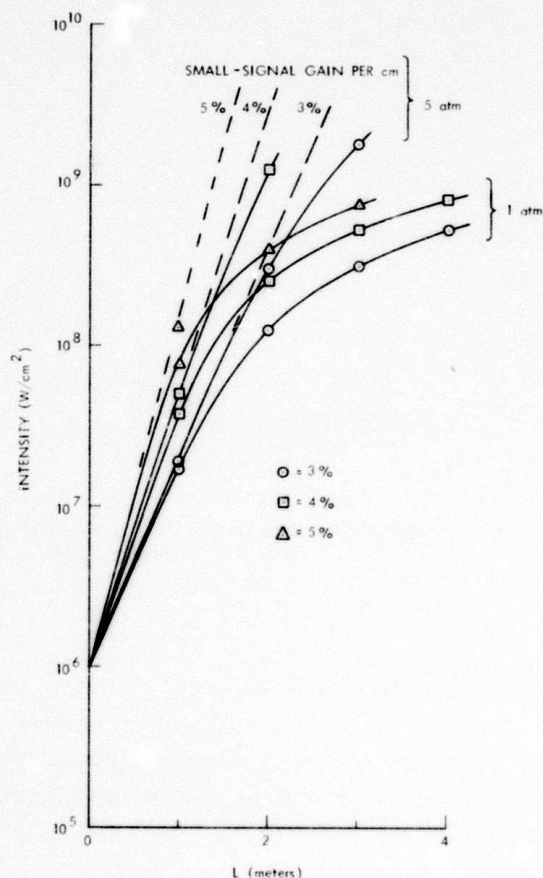


Fig. VI-10. Peak intensity of amplified short pulse in  $\text{CO}_2$  media of known small-signal gain at 1 and 5 atm total pressure. Gas mixture: 0.30:0.05:0.65 ( $\text{CO}_2:\text{N}_2:\text{He}$ ). Input pulse: Gaussian shape, 1 ns FWHM, peak intensity  $10^6 \text{ W/cm}^2$ .



## (VI. APPLIED PLASMA RESEARCH)

illustrated; these are typical of those to be expected in various high-pressure discharges. Peak pulse intensity as a function of depth in the amplifier is shown in Fig. VI-10, and the output pulse shapes are shown in Fig. VI-11.

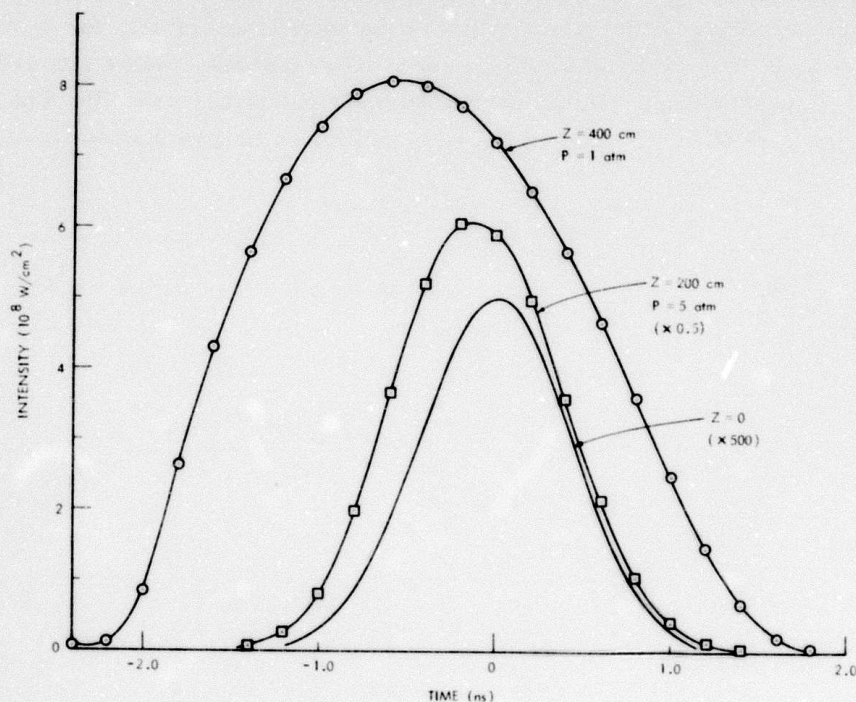


Fig. VI-11. Temporal pulse profiles for amplifiers of Fig. VI-10, 4%/cm small-signal gain at 1 atm, 3%/cm at 5 atm.

Note that there is substantial broadening of the pulse at 1 atm, while at 5 atm the output is a reasonably faithful duplicate of the input, even after amplification by more than 1000 in intensity. Note also the extremely large saturation intensity at 5 atm; elementary considerations of the saturation process show that it should scale approximately as the square of the total pressure.

## References

1. F. A. Hopf and C. K. Rhodes, "Influence of Vibrational, Rotational, and Reorientational Relaxation on Pulse Amplification in Molecular Amplifiers," *Phys. Rev. A* **8**, 912-929 (1973).
2. A. I. Osipov and E. V. Stupochenko, "Non-equilibrium Energy Distributions over the Vibrational Degrees of Freedom in Gases," *Sov. Phys. -Usp.* **6**, 47-66 (1962).



APPENDIX IV

Preprint: to appear in the Journal of Quantum Electronics

H. A. Haus, "A Theory of Forced Mode Locking"

## A THEORY OF FORCED MODE LOCKING\*

by H. A. Haus\*\*

### Abstract:

A theory of forced mode locking is set up on the basis of an expansion of the electromagnetic fields in the optical cavity in terms of the cavity modes. Mode locking is viewed as injection locking of the cavity modes via generation of frequency sidebands by the mode locking element. The approach leads naturally to simplifying assumptions that are legitimate in most practical cases. In the case of a homogeneously broadened laser medium, a simple differential equation is obtained for the mode locked pulse train for an arbitrary periodic mode locking modulation. The analogy of the equation with well known solved problems of quantum mechanics is used to determine the nature of the solutions. For any given modulation, usually more than one mode locked solution is found. In the case of sinusoidal modulation, one of the solutions reduces to that previously derived by Siegmann and Kuizenga. The higher order solutions are shown to be unstable. The case of mode locking of an inhomogeneously broadened laser medium is solved.

---

\* Work supported by Joint Services Electronics Program (Contract DAAB07-71-C-0300). US Army Research Office - Durham (Contract DAHC04-72-C-0044).

\*\* Electrical Engineering Department and Research Laboratory of Electronics, Massachusetts Institute of Technology, Cambridge, Mass. 02139.

## Introduction

The theoretical investigations of mode locking[see Ref. 1 for a large list of references] may be roughly divided into two groups, (a) those which treat the mode locking process in the time domain, e.g. the paper by Kuizenga and Siegman[2], and (b) those which treat the phenomenon in the frequency domain (notably the paper by McDuff and Harris[3]). In this paper we present a useful extension of the mode locking analysis in the frequency domain. When setting up the analysis of saturable absorber mode locking by a somewhat novel approach we soon discovered that this approach lent itself very well to a better understanding of the forced mode locking phenomenon and permitted the solution of previously unsolved problems of mode locking theory.

This paper is devoted to forced mode locking. In particular the following issues are addressed: 1. Mode locking of a homogeneously broadened laser by sinusoidal amplitude modulation. Well known results are obtained, but this part of the paper is intended mainly to show the correspondence with previous work. 2. Mode locking by sinusoidal amplitude modulation of an inhomogeneously broadened laser. 3. Modulation, other than sinusoidal, of a homogeneously broadened laser. 4. Stability of the mode locked pulses of a homogeneously broadened laser.

The presentation of a theory of mode locking from a different point of view needs some justification in view of the

large literature on the subject. It is believed that the approach presented here offers the following advantages:

(a) The theory of coupled oscillators is a well known one and offers insights which are not as easily obtained using the approach of pulse propagation through nonlinear media.

(b) The theory of injection locking has been recently discussed very lucidly[4]. The analysis of the stability of locked oscillators can be transferred almost unchanged to the treatment of the stability of mode locked pulse trains.

(c) Simplifying assumptions concerning the character of the laser medium are suggested by the new approach which lead to very simple differential equations. The very simplicity of these differential equations then allows the treatment of problems not hitherto attempted. The present paper illustrates two such applications: mode locking of an inhomogeneously broadened laser and stability analysis of the mode locked pulse train.

## I. Mode Locking as Injection Locking

Injection locking of a cavity with a single mode containing a negative conductance may be analyzed with the aid of the equivalent circuit of Fig. 1. Here the admittance  $Y_L(|V|)$  represents the active admittance of the gain element which is in general complex and a function of the magnitude of the complex voltage  $V$ , and  $Y_C$  is the cavity admittance, a function of  $\omega$ . If a current source  $I_S$  of frequency  $\omega$  is applied across the circuit as indicated, then the equation for this injection locked oscillator is given by

$$I_S = [Y_C(\omega) + Y_L(\omega, |V|)] V \quad (1.1)$$

Equation (1.1) can be adapted to the case of a mode locked optical cavity involving the interaction among many axial modes. The identification of equivalent circuit elements of each resonance circuit (representing one axial laser mode) with laser and optical cavity parameters is carried out in Appendix I.

The electric field in the cavity is expanded in the set of axial modes of the empty cavity, with mode pattern  $\bar{e}_k(\bar{r})$ ; the expansion coefficients become the voltages  $V_k$  of the different resonance circuits. One assumes at the outset that mode locking is successful and that all modes oscillate near their respective resonance frequencies. The frequency separation of the oscillations is dictated by the injection signals which are by definition separated by  $\omega_M$ , the frequency of the mode locking element.

Whether or not the solutions thus found are physically acceptable, i.e. stable, and the starting assumption of 'successful mode locking is indeed justified, must be left for a stability analysis which is carried out at the end of the paper.

These assumptions imply that the electric field in the cavity can be expanded as follows:

$$\bar{E}(\bar{r}, t) = e^{j\omega_0 t} \sum_k V_k e^{jk\omega_M t} \bar{e}_k(\bar{r}) + \text{c.c.} \quad (1.2)$$

where the  $k$ -th mode has the frequency

$$\omega_k = k \omega_M + \omega_0. \quad (1.3)$$

The fast time dependence  $\exp^{j\omega_0 t}$  has been explicitly extracted where  $\omega_0$  is to be identified with the frequency of the central mode ( $k = 0$ ), the mode nearest to the peak of the laser gain profile (peak of the negative conductance  $\text{Re } Y_L$ ).

Each complex amplitude  $V_k$  obeys a set of equations that can be summarized in a parallel equivalent circuit. The equivalent circuits describing different modes are coupled by the side-band generation of the mode locking element, i.e. the driving current for the  $k$ -th cavity mode,  $I_{Sk}$ , contains contributions of  $V_i$  ( $i \neq k$ ). We shall disregard couplings as caused by other effects. Thus, in particular, we shall assume that the gain of the laser medium (represented by  $Y_L$ ) is time independent and

therefore no sidebands are produced on frequency components amplified by the laser medium. This in turn implies that the population relaxation time  $T_1$  is long compared with the cavity transit time so that the laser medium, while affected by the time average optical power in the cavity, does not respond to instantaneous power fluctuations. (This assumption was also made in Ref. 2.) Generalizing (1.1) to the  $k$ -th cavity mode with amplitude  $V_k$  one has:

$$[Y_{Ck}(\omega_k) + Y_L(\omega_k)] V_k = I_{Sk} \quad (1.4)$$

Consider first the dependence of  $Y_{Ck}(\omega_k)$  upon  $\omega_k$ . The  $k$ -th cavity mode has a quality factor  $Q$  (assumed to be the same for all modes) and a resonance frequency

$$\omega_{k0} = k \Delta\omega + \omega_0 \quad (1.5)$$

where  $\Delta\omega$  is the separation between the resonances of the (empty-axial) cavity modes. Since the frequency of excitation is given by (1.3), one has

$$Y_{Ck} = G_C \left[ 1 + kj 2Q \frac{\omega_M - \Delta\omega}{\omega_0} \right]. \quad (1.6)$$

Next, consider  $I_{Sk}$  of (1.4). If the cavity is mode locked by the time dependent loss of a mode locking element, then

$$I_{Sk} = - G_C \left[ m(t) \sum_l v_l e^{jl\omega_M t} \right]_{k\text{-th Fourier component}} \quad (1.7)$$

where  $m(t)$  has the time dependence of the loss modulation (with period  $2\pi/\omega_M$ ) and its magnitude is a measure of the "loading" of the cavity by the mode locking element. (See Appendix I for details.)

In (1.7) all modes  $l$  affect the mode  $k$  equally ( $m(t)$  is  $k$  and  $l$  independent) an assumption justified if the mode locking element is near one of the mirrors. Other positions of the mode locking element must be handled differently as shown in Section V. The expression (1.7) may also be written,

$$I_{Sk} = - G_C \sum_l M^{(k-l)} v_l \quad (1.8)$$

where  $M^{(k-l)}$  is the  $(k-l)$ -th Fourier component in the Fourier decomposition of  $m(t)$ ;

$$m(t) = \sum_k M^{(k)} e^{jk\omega_M t}. \quad (1.9)$$

Combining (1.4), (1.6), and (1.7) we obtain

$$G_C \left[ 1 + k j 2Q \frac{\omega_M - \Delta\omega}{\omega_0} \right] v_k + Y_L(\omega_k) v_k = - G_C \left[ m(t) \sum_l v_l e^{jl\omega_M t} \right]_{k\text{-th component}} \quad (1.10)$$



Finally, consider the admittance of the laser medium (for details, see Appendix I). The laser gain is frequency dependent, and a Lorentzian line shape will be assumed. The admittance may be normalized to  $G_C$  so that

$$Y_L(\omega_k) = -G_C \frac{g}{1 + j \frac{\omega_k - \omega_0}{\omega_L}} \quad (1.11)$$

where  $\omega_L$  is the laser medium linewidth, and  $g$  is the magnitude of the negative conductance at line center normalized to  $G_C$ . We have assumed that the center frequency of the laser line coincides with one of the cavity mode oscillations. If the mode spectrum is dense as it must be to get good mode locking, this is not a serious restriction.

We shall now make the most important assumption of this study, which, in fact, is the assumption crucial for obtainment of the simple equations of this treatise. We assume that (1.11) can be expanded in  $\omega_k - \omega_0/\omega_L$  and only terms up to second order are retained

$$Y_L(\omega_k) \approx -G_C g \left\{ 1 - \left( \frac{\omega_k - \omega_0}{\omega_L} \right)^2 - j \frac{\omega_k - \omega_0}{\omega_L} \right\} \quad (1.12)$$

This assumption implies that the pulse widths predicted by the ensuing analysis must be long compared with  $1/\omega_L$ . This assumption is usually justified in practice.

The conductance  $g$  is power dependent. If one normalizes the field pattern  $\bar{e}_k$  appropriately, the power  $P$  on the traveling waves of the (standing wave) modes propagating in one axial direction can be set equal to

$$P = \sum_k |V_k|^2 \quad \text{and} \quad g = \frac{g_0}{1 + \frac{P}{P_L}} \quad (1.13)$$

for a homogeneously broadened medium;  $P_L$  is the saturation power of the laser medium in general a function of  $\omega_k$ . If the pulse spectrum is narrow, as assumed, the  $\omega$ -dependence can be disregarded. (1.12) is correct strictly speaking only if all modes act on the laser medium in an identical way, i.e. if the medium is concentrated near one of the mirrors. The phenomenon of "spatial hole burning" is thus excluded. Assumption (1.12) may not be too restrictive even for a laser medium occupying a larger portion of the cavity length.

Suppose at first that

$$m(t) = 2M[1 - \cos \omega_M t] \quad (1.14)$$

the modulation is purely sinusoidal. Then

$$I_{Sk} = G_C M[V_k - 1 - 2V_k + V_{k+1}]. \quad (1.15)$$

Adhering to this example, and introducing (1.15), (1.3), (1.5) and (1.12) into (1.10) we obtain the second order difference equation:

$$\left\{ 1 - g \left[ 1 - \left( \frac{k \omega_M}{\omega_L} \right)^2 \right] + j \frac{k \omega_M}{\omega_L} \left( 2Q \frac{\omega_M - \Delta\omega}{\omega_M} \frac{\omega_L}{\omega_0} + g \right) \right\} v_k$$

$$= M[v_k - 1 - 2v_k + v_{k+1}].$$

(1.16)

## II. Solution of Sinusoidal Mode Locking of Homogeneously Broadened Laser

We make a further approximation so as to enable us to find simple solutions to the difference equation (1.16). If many modes are to be locked, and if the variation of the gain over a frequency range corresponding to the mode spacing is small, then the difference equation can be replaced by a second order differential equation. One has

$$\left[ v_k + 1 - 2v_k + v_k - 1 \right] + \omega_M^2 \frac{d^2 v}{d\omega^2}$$

where  $v_k$  is now replaced by a continuous function of the variable  $\omega$ , the frequency deviation from  $\omega_0$ , and  $\omega_M$  is the frequency separation of the spectral lines. The modes are identified by the continuous variable  $\omega = \lim_{k \rightarrow \infty} k \omega_M$ , where  $k$  is the mode number, which assumes  $\omega_M \rightarrow 0$  both positive and negative values. One obtains for (1.16) [5]:

$$\left[ 1 - g \left( 1 - \frac{\omega^2}{\omega_L^2} \right) + j \frac{\omega}{\omega_L} (\delta + g) \right] v = M \omega_M^2 \frac{d^2 v}{d\omega^2} \quad (2.1)$$

where  $\delta$  is a measure of cavity "detuning", proportional to the difference between the modulation frequency and cavity resonance frequency spacing:

$$\delta = \frac{\omega_M - \Delta\omega}{\omega_M} 2Q \frac{\omega_L}{\omega_0} \quad (2.2)$$

Eq. (2.1) is particularly simple, if we require that

$$\delta + g = 0. \quad (2.3)$$

This implies that

$$\omega_M - \Delta\omega = - \frac{1}{2Q} g \frac{\omega_M \omega_0}{\omega_L} \quad (2.4)$$

The modulation frequency deviates from the cavity frequency by an amount proportional to the laser medium dispersion. In fact, (2.4) means that the modulation frequency is adjusted to equal the cavity mode frequency separation as modified by the laser medium. Hence (2.4) may be viewed as excitation by a modulation tuned to the actual mode separation, i.e. resonant modulation. With (2.3) satisfied, (2.1) has a pure real coefficient on the right hand side. The resulting equation is identical with the harmonic oscillator equation of quantum mechanics, where  $V$  plays the role of the wave function and  $\omega$  the role of the spacial variable.

$$\left[ 1 - g \left( 1 - \frac{\omega^2}{\omega_L^2} \right) \right] V = M \omega_M^2 \frac{d^2 V}{d\omega^2} \quad (2.5)$$

We can now bring to bear the entire formalism of the quantum mechanical harmonic oscillator on the problem of loss modulation in a homogeneously broadened medium. The solutions of (2.5) are

the well known Hermite gaussians[6]

$$V(\omega) = H_n \left( \frac{\omega}{\omega_P} \right) \exp - \frac{1}{2} \left( \frac{\omega}{\omega_P} \right)^2 \quad (2.6)$$

where

$$\omega_P = \sqrt{\frac{M}{g}} \sqrt{\omega_L \omega_M} . \quad (2.7)$$

The role of the energy eigenvalues  $E_n$  of the harmonic oscillator is played by the parameter  $g - 1$  in (2.5). We find for the quantization of this parameter

$$E_n = g - 1 = \frac{2 \sqrt{Mg} \omega_M (n + 1/2)}{\omega_L} \quad (2.8)$$

Equation (2.6) defines "supermodes" or "mode locking modes" of the mode locked oscillator. The higher the order  $n$  of the "supermode", the more structure in the frequency spectrum. Since the Fourier transform of the spectrum (2.6) leads to the same time dependence, we find that mode locked solutions may exist of higher and higher temporal structure exhibiting more and more pulses. The lowest order supermode was obtained by Siegman and Kuizenga[2] and the higher order supermodes by Haken and Pauthier[7] and others[8,9]. We shall show in Section VI that all higher order supermodes ( $n > 0$ ) cannot be excited in the

steady state because they are unstable. Equation (2.8) determines the power in the mode locked cavity. Indeed by solving for  $g$  from (2.8) and then using the dependence of  $g$  upon power  $P$ , (1.13), we find the following relationship for  $P$ :

$$\frac{P}{P_L} = \frac{g_0}{1 + \mu + \sqrt{2\mu + \mu^2}} - 1 \quad (2.9)$$

$$\text{where } \mu = \frac{1}{2} (2n + 1)^2 M \left( \frac{\omega_M}{\omega_L} \right)^2$$

In the limit of a small modulation coefficient  $M$ , (2.9) becomes

$$\frac{P}{P_L} = g_0 - 1 - 2g_0 \sqrt{M} \frac{\omega_M}{\omega_L} (n + 1/2) \quad (2.10)$$

Let us now return to an interpretation of the present solution in terms of the physical model used as a starting point of the investigation, the injection locking model. We must remember that the differential equation was used as a mathematical approximation to the difference equation, and that the solution obtained must be interpreted as an approximate solution of the difference equation if the replacement is made:  $V(\omega) \rightarrow V_k$  and the solution (2.6) is assigned values only at discrete frequencies  $\omega_k$ . Mode locking has led to simultaneous oscillation of many modes in a homogeneously broadened system, even though the unmodulated



system would have oscillated only in a single mode. The simultaneous oscillation in many modes is allowed because of injection locking. The injection currents are

$$I_{Sk} = G_C M \left[ V_{k-1} - 2 V_k + V_{k+1} \right].$$

Figure 2 shows a plot of the real part of the two sides of (1.16) vs  $\omega_k$  (the imaginary part vanishes because of assumed resonant modulation), showing explicitly the discrepancies  $\text{Re}[Y_C(\omega_k) + Y_L(\omega_k)]$  which are balanced by the modulation-produced "source" current normalized to the oscillation voltage,  $I_{Sk}/V_k$ .

The results obtained thus far are well known. One can extend our expressions to cover reactive (phase) rather than loss (amplitude) modulation by replacing  $M$  by an imaginary quantity, again arriving at results derived previously. The mathematical steps necessary for such modifications are interesting, but are not presented here because no new results are obtained[10]. Instead, we shall concentrate here on problems whose solutions were not obtained previously.

### III. Inhomogeneously Broadened Medium

If the medium is inhomogeneously broadened, then the power in any particular cavity mode determines the pulldown of the gain line at that particular cavity frequency (provided, of course, that the separation of the cavity modes is large compared with the homogeneous linewidth of the medium). The adaptation of (2.1) to the case of an inhomogeneously broadened medium is accomplished by changing the character of the dependence of the negative conductance  $g$  upon intensity. To first order, the reactive contribution is unaffected by saturation. The equation is:

$$\left[ 1 - \frac{g_0 \left( 1 - \frac{\omega^2}{\omega_L^2} \right)}{\sqrt{1 + \frac{|V|^2}{P_L}}} + j \frac{\omega}{\omega_L} (\delta + g_0) \right] V = M \omega_M^2 \frac{d^2 V}{d\omega^2} \quad (3.1)$$

where  $P_L$  is a conveniently defined saturation intensity. Eq. (3.1) is a nonlinear differential equation for the voltage  $V$ . It is a difficult equation to solve; yet it is possible to gain considerable insight into the nature of its solutions by giving it a physical interpretation. Let us separate the complex voltage amplitude into an amplitude and a phase factor

$$V = A e^{j\phi} \quad (3.2)$$

Taking the second derivative of (3.2) one obtains

$$\frac{d^2 V}{d\omega^2} = \ddot{A} e^{j\phi} + 2j\dot{\phi} \dot{A} e^{j\phi} + j\ddot{\phi} A e^{j\phi} - \dot{\phi}^2 A e^{j\phi} \quad (3.3)$$

Introducing (3.2) and (3.3) into (3.1) one has

$$M \omega_M^2 (\ddot{A} - \dot{\phi}^2 A) = \left\{ 1 - \frac{g_0 \left[ 1 - \frac{\omega^2}{\omega_M^2} \right]}{\sqrt{1 + \frac{A^2}{P_L}}} \right\} A \quad (3.4)$$

$$M \omega_M^2 (A\ddot{\phi} + 2\dot{A}\dot{\phi}) = \frac{\omega}{\omega_L} (\delta + g_0) A \quad (3.5)$$

Here we have written  $(\dot{\phantom{x}})$  for  $d/d\omega$  in order to emphasize the analogy with the equations of motion of a particle in polar coordinates; the frequency variable plays the role of "time", the amplitude  $A$  is analogous to "radius". The force field is "radius" and "time" dependent. If one assumes that the driving frequency is matched to the frequency separation of the cavity modes as modified by the medium, then  $\delta + g_0 = 0$  and the force field becomes a central one. In this case, one may define a potential function, the derivative of which gives the force. The potential function plotted against "radius"  $A$  as a function of "time"  $\omega$  is shown in Figure 3. The potential hill travels as a function of time towards the origin and then the origin becomes

a hill in its own right. If one looks for a mode locked "super-mode", one looks for the motion of a particle that starts with zero velocity at a time  $t = 0$  (zero slope at center frequency), and then approaches the origin ( $A = 0$ ) where it comes to a full stop.

Consider first the case in the absence of modulation. In the particle motion analog, this corresponds to a massless particle. The particle "looks" for a position in which it is exposed to zero force field. The particle stays at the top of the hill starting infinitesimally to the left and then searches for the position in which the force is infinitesimally small yet directed from right to left. When the potential hill has made it to the origin, the particle has followed it there and then stays there forever. This case can be solved very simply analytically by setting the righthand side of equation (3.4) = 0.

Consider next the case when there is modulation, at first the case of very small mass (modulation). Near  $t = 0$ , when the force field is strong, the particle seeks out positions in the potential field at which it is exposed to a small force to the left. This means that the particle starts to the left of the hill at  $t = 0$ , i.e. at a smaller radius than the massless particle. In the language of mode locking, this corresponds to a power of the mode near line center that is smaller than the power in the absence of mode locking. Near the origin, the particle has acquired a finite velocity and kinetic energy. In order to come to a full stop at the origin, it has to expend the kinetic

energy by climbing up a hill. This means that, before the particle comes to full rest, the origin must have already risen above its surroundings. Translated into the language of the mode locked "mode" this means that the frequency bandwidth of the mode is wider than in the absence of modulation (in the language of the equivalent particle the origin of the radial coordinate develops into a hill before the massless particle has reached the origin).

The model is useful also for determining what happens when the strength of mode locking is increased excessively. This corresponds to a very massive particle. The potential, as defined, does not involve the mode locking amplitude  $M$  and hence, in the equivalent language of the particle, the initial hill becomes smaller, the heavier the particle. A supermode, symmetric at line center, corresponds to an initial condition for the analog particle starting at rest to the left of the potential hill. A particle which starts initially at rest slightly to the left of the potential hill may be too massive to make it near the origin before the potential distribution has changed beyond recall, preventing the particle from acquiring sufficient kinetic energy. The particle never makes it to the origin. No solution exists for excessively high values of  $M$ .

There are also higher order solutions, if the modulation is not too strong. One may start the particle on the down slope of the hill. (Note the peak intensity at center frequency for this mode is less than for the lowest order supermode.) The particle may go through the origin and climb up the hill on the other side.

After oscillating back and forth, the particle can be brought to rest at the origin. Such solutions exist only for particles of finite mass (i.e. finite modulation).

Equation (3.4) has two adjustable parameters,  $g_0 - 1$ , the excess small signal gain at line center ( $\omega = 0$ ) and the normalized modulation parameter  $\sqrt{\frac{M}{g_0}} \frac{\omega_M}{\omega_L}$ . For a range of these two parameters, solutions for the particle motion were obtained. Figure 4 shows plots of  $A/\sqrt{P_L}$  vs normalized frequency  $\omega/\omega_M$ , for various choices of the parameters  $\sqrt{\frac{M}{g_0}} \frac{\omega_M}{\omega_L}$  and  $g_0 - 1$ . Figure 5 shows the range in the  $(g_0 - 1)$ ,  $\sqrt{\frac{M}{g_0}} \frac{\omega_M}{\omega_L}$  plane over which mode locked solutions are obtained. Figure 6 shows the decrease of the oscillation amplitude at line center  $A(0)/\sqrt{P_L}$ , as a function of normalized modulation, for different excess small signal gains.

#### IV. General Time Dependent Loss Modulation

The generalization to a general, time dependent, loss modulation calls for re-examination of the "injection current" expression (1.7). This expression suggests that an analysis of the mode locking problem in the time domain may lead to simplifications. Indeed, if one defines

$$i_S(t) \equiv \sum I_{Sk} e^{jk\omega_M t} \quad (4.1)$$

one finds

$$I_S(t) = - G_C m(t) \underline{v}(t) \quad (4.2)$$

where  $\underline{v}(t) = \sum_{\ell} v_{\ell} e^{j\ell\omega_M t}$  is the time dependent amplitude of the electric field near one of the mirrors. Equation (4.2) states simply that the time dependent source current is the product of the modulated time dependent conductance  $G_C m(t)$  and the field amplitude.

All of this is straight forward and would not profit us very much if one could not transform the left hand side of (1.4) into the time domain and obtain a simple result. In general, this is not possible. However, with the approximations already made for  $Y_C(\omega_k)$  and  $Y_L(\omega_k)$  we may carry out the transformation and obtain a very simple result. Using the same approximations that led to (1.6), one obtains in the time domain:



$$\left\{ 1 - g \left[ 1 + \frac{1}{\omega_L^2} \frac{d^2}{dt^2} \right] + (g + \delta) \frac{d}{dt} \right\} v(t) = m(t) v(t) \quad (4.3)$$

In the case of "resonant" excitation,  $g + \delta = 0$ , one obtains a differential equation in time for  $v(t)$  with a simple quantum mechanical analog. A particle with the mass  $2m/\hbar^2 = \omega_L^2/g$  moves in the potential well  $m(t)$  where the role of the spatial variable  $x$  of quantum mechanics is now played by the time. The sinusoidal modulation problem of the homogeneously broadened laser could have been solved in the time domain, with  $1 - \cos \omega_M t \rightarrow \frac{1}{2}(\omega_M t)^2$  and the hermite gaussian solutions would have been obtained, another way of observing the invariance of hermite gaussians with regard to Fourier transformation. Note, however, that a solution of the inhomogeneously broadened laser mode locking problem would have been difficult in the time domain.

Solutions of (4.3) can be obtained once one assumes special forms of the modulation function. Consider for example a very deep modulation of the mode locking crystal which shuts off transmission entirely outside an interval of length  $\tau$ . This is shown in Figure 7. Equation (4.3) for the square potential well is the quantum mechanical problem of an electron in a perfectly reflecting box. The eigenfunctions and eigenvalues of this problem are well known and are

$$V(t) = \cos \frac{n\pi}{\tau} t \quad (4.4)$$

in the time domain. The eigenvalues are

$$g - 1 = \frac{g}{\omega_L^2} \left( \frac{n\pi}{\tau} \right)^2. \quad (4.5)$$

In the time domain the mode locked pulse is entirely confined to the time period of length  $\tau$ .

If the square wave modulation is modified to one of lesser depth, one has the problem of an electron in an open square well with well known eigenfunctions [6].

One may think of many other modulation forms for all of which it is easy to arrive at qualitative conclusions as to the shape of the mode locking pulse and the possibility of mode locking.

The viewing of the mode locking problem in the time domain affords other insights. Consider for example the question as to what approximations were made when the discrete spectrum of the cavity oscillations was replaced by a continuum and the modulation of loss, which was sinusoidal, was replaced by the operator  $d^2/d\omega^2$ . In the time domain, this operator is replaced by the function  $-\frac{1}{2}t^2$ . If one considers the periodic problem, one has to make two modifications: (a) one must return to the full time dependence of the modulation and replace, in the time domain, the parabola by the cosine function. (b) One must look for solutions of the time dependent problem which are periodic.

Clearly the introduction of a periodic modulation function in lieu of the parabolic one, introduces a periodic well in time

space. The problem is now a quantum mechanical problem in a periodic potential. If the modulation is strong enough so that the eigenvalues lie near the bottom of the well, one obtains a set of solutions in each of the well bottoms, which is almost the same gaussian solution that has been obtained previously. The eigenfunction consists of isolated pulses in time, repeating periodically. On the other hand when the modulation decreases, the walls of the periodic wells decrease and for a given strength of modulation, solutions are found with overlap between the wave functions within each of the periodic wells. The mode locking is not strong enough to suppress the amplitude between pulses.

### V. General Position of Mode Locking Element

When the mode locking element is moved a distance  $z_0$  away from one mirror, where  $\omega_p z_0/c$  is comparable to one or larger, one may not assume that the modes of interest have roughly the same field patterns throughout the mode locking element.

If the time varying conductivity of the mode locking element is  $\sigma_M(\bar{r}, t)$ , the injected current  $I_{Sk}$  is proportional to

$$- \sum_l \int \sigma_M(\bar{r}, t) \bar{e}_k^* \cdot \bar{e}_l dv V_l e^{j l \omega_M t} \Big|_{k\text{-th Fourier component}}$$

and  $m(t)$  of (1.7) has to be replaced by an expression proportional to

$$m_{kl}(t) \propto \int \sigma_M(\bar{r}, t) \bar{e}_l \cdot \bar{e}_k^* dv$$

which depends on  $k$  and  $l$ . Now

$$\bar{e}_k \propto \sin \frac{(k \Delta\omega + \omega_0) z}{c}$$

and using a corresponding expression for  $\bar{e}_l$ , one finds that  $\bar{e}_k^* \cdot \bar{e}_l$  contains some rapidly spatially varying terms, which integrate out to zero and a more slowly varying term

$$\frac{1}{2} \left[ \exp j(k - l) \frac{\Delta\omega}{c} z + \exp - j(k - l) \frac{\Delta\omega}{c} z \right]$$

Spatial integration over the "short" mode locking element replaces  $z$  by  $z_0$ , where  $z_0$  is the position of the element measured from one mirror. The injection current  $i_s(t)$  in the time domain, as defined by (1.8), becomes

$$i_s(t) = \sum_k I_{Sk} e^{jk\omega_M t} = \frac{1}{2} \sum_{k,i} M(k-i) e^{jk\omega_M t} \left[ \exp j(k-i) \frac{\Delta\omega}{c} z_0 + \exp j(i-k) \frac{\Delta\omega}{c} z_0 \right] = \frac{1}{2} \left[ m \left( t - \frac{\Delta\omega}{\omega_M} \frac{z_0}{c} \right) + m \left( t + \frac{\Delta\omega}{\omega_M} \frac{z_0}{c} \right) \right] v(t).$$

The time dependent injection signals are produced by the delayed and advanced versions of the mode locking modulation, a very obvious result. What is remarkable, however, is that we may now effect a simple generalization of the results of the preceding section to obtain the mode locking solutions for this problem. Suppose we have a square wave modulation as shown in Figure 8. If the time delay (advance)  $\frac{\Delta\omega}{\omega_M} \frac{z_0}{c}$  is one quarter of the period of  $\omega_M$  (center of the cavity,  $\Delta\omega \approx \omega_M$ ) the number of potential wells has doubled as shown in Figure 8 but their depth has decreased. The number of mode locked pulses doubles provided the depth of the wells is still sufficient to allow "trapped" solutions. If the modulation is of a more general shape, displacement of the element causes variations in the shape of the effective potential well, leading to distortions in the wave function (pulse shape). The present approach can be used to ascertain pulse shapes in a

standing wave cavity with the mode locking element not near one of the mirrors.

## VI. Stability of Solutions of Homogeneously Broadened Laser Medium

In this section we study the stability of the supermodes with respect to arbitrary perturbations. We shall follow the analysis of stability of injection locking of Kurokawa[4]. In this analysis, the assumed steady state is perturbed, the perturbation is taken to be a slow function of time (compared with the time variation of the unperturbed oscillation).

An instantaneous frequency and growth or decay rate is obtained for the perturbation and the transient time evolution of the perturbation is studied for net growth or decay. If it can be shown that there is no net growth the injection locking is stable, otherwise it is unstable.

We shall extend this analysis to the study of the stability of "steady state" mode locking solutions. Here all oscillations are coupled to each other through the injection locking process. The stability study is concerned with the time evolution of these coupled perturbations.

Study of transients implies the replacement of the frequencies  $\omega_k$  of the modes by  $\omega_k + \Omega_k$  where  $\Omega_k$  is complex;  $-\text{Im}(\Omega_k) > 0$  implies growth of excitation. Further the "instantaneous" perturbation frequency  $\Omega_k$  itself is a function of time. Thus even temporary growth may be offset by eventual decay.

The objective then is to obtain an equation for a complex perturbation  $\delta V_k$  of the steady state  $V_k$  and the frequency  $\Omega_k$  of the perturbation which is, in general, a function of the



phase  $\phi_k$  between  $\delta v_k$  and  $v_k$ . The perturbation obeys the same difference equation (1.16) as  $v_k$ , except that  $\Omega_k$  must be replaced everywhere by  $\omega_k + \Omega_k$  and  $g$  may be perturbed because an amplitude perturbation changes  $P$  and thus changes  $g$ . All  $\omega_k$  dependent parameters may be expanded to first order in the  $\Omega_k$ 's if the  $\Omega_k$ 's are assumed small (small growth rates and frequency deviations).

We shall disregard all derivatives of the parameters of (1.4) with respect to  $\Omega_k$ , except that of  $\text{Im } Y_{Ck}(\omega_k)$ . This is tantamount to disregarding all energy storages other than the electromagnetic energy storage of the cavity modes. If the oscillation of the perturbation  $\delta v_k$  of the  $k$ -th axial mode occurs with the frequency  $\omega_k + \Omega_k$ , then the admittance to be associated with  $\delta v_k$  is

$$Y_{Ck}(\omega_k + \Omega_k) = Y_{Ck}(\omega_k) + j \Omega_k \frac{2Q}{\omega_k}$$

or in the continuum limit

$$Y_C(\omega + \Omega) = Y_C(\omega) + j\Omega \frac{2Q}{\omega_0} \quad (6.1)$$

If we assume that the unperturbed solution is the  $n$ -th supermode,  $V_n(\omega)$ , excited at synchronism (i.e.  $g + \delta = 0$ ) expand the difference equation as indicated and go to the continuum limit, we obtain the equation:

$$\left[ M \omega_M^2 \frac{d^2}{d\omega^2} + g \left( 1 - \frac{\omega^2}{\omega_L^2} \right) - 1 \right] \delta V$$

$$+ (\delta g) \left( 1 - \frac{\omega^2}{\omega_L^2} - j \frac{\omega}{\omega_L} \right) V_n = \frac{2Q}{\omega_0} j\Omega \delta V \quad (6.2)$$

Next, consider the perturbation  $V_n \delta g$ .

$$V_n \delta g = V_n g_0 \delta \left( \frac{1}{1 + \frac{P}{P_L}} \right) = - \frac{V_n g_0}{\left( 1 + \frac{P}{P_L} \right)^2} \delta \left( \frac{P}{P_L} \right) \quad (6.3)$$

If the voltage  $V_n(\omega)$  is so normalized that  $\int |V_n(\omega)|^2 d\omega$  is equal to the power, then

$$\delta P = \int |V_n(\omega) + \delta V(\omega)|^2 d\omega - \int |V_n(\omega)|^2 d\omega = 2 \int V_n(\omega) \operatorname{Re} \delta V d\omega \quad (6.4)$$

and thus we obtain for (6.2)

$$\left[ M \omega_M^2 \frac{d^2}{d\omega^2} + g - 1 - \frac{g\omega^2}{\omega_L^2} \right] \delta V - 2 \left( 1 - \frac{\omega^2}{\omega_L^2} - j \frac{\omega}{\omega_L} \right) \frac{V_n g}{1 + \frac{P}{P_L}} \frac{\int V_n(\omega) \operatorname{Re} \delta V d\omega}{P_L}$$

$$= \frac{2Q}{\omega_0} j\Omega \delta V \quad (6.5)$$

It is convenient to test first the stability of a general  $n$ -th supermode with respect to a perturbation  $\delta V(\omega)$  proportional to the  $m$ -th supermode,  $\delta V(\omega) = a_m u_m(\omega)$ , and study the frequency  $\Omega(\omega)$  of the perturbation; here  $u_m(\omega)$  is a properly normalized eigenfunction of the defining equation of the supermodes

$$\left[ M \omega_M^2 \frac{d^2}{d\omega^2} - g \frac{\omega^2}{\omega_L^2} \right] u_m = - E_m u_m \quad (6.6)$$

and the eigenvalues  $E_m$  are given by (2.8). Since the eigenfunctions are orthogonal, we may set

$$\int_{-\infty}^{\infty} u_n u_m d\omega = \delta_{nm}. \quad (6.7)$$

Introducing  $\delta V = a_m u_m(\omega)$  in (6.5) and using the orthogonality condition, we obtain for the frequency deviation:

$$\Omega = j \frac{\omega_0}{2Q} (E_m - E_n) \quad (6.8)$$

For  $E_m < E_n$ , i.e. for  $m < n$ , one obtains  $\text{Im}\Omega < 0$  and one finds growth of the perturbation. Thus any  $n$ -th supermode is unstable with respect to a perturbation having a dependence upon cavity mode number  $(\omega)$  corresponding to a lower order supermode. Hence all modes  $n > 0$  are unstable.

The only possible stable mode is the 0-th order (gaussian) mode. In order to prove its stability we must show that a general

perturbation  $\delta V = \sum_m a_m u_m(\omega)$  does not lead to exponential growth. We find from (6.5), using  $V_0(\omega) = \sqrt{P} u_0(\omega)$

$$\begin{aligned}
 & - \sum_m (E_m - E_0) a_m u_m(\omega) - \frac{g \frac{P}{P_L}}{1 + \frac{P}{P_L}} 2 \operatorname{Re} a_0 \left( 1 - \frac{\omega^2}{\omega_L^2} - j \frac{\omega}{\omega_L} \right) u_0(\omega) \\
 & = 2 \frac{Q}{\omega_0} j \Omega \sum_m a_m u_m(\omega)
 \end{aligned} \tag{6.9}$$

Through multiplication by  $u_m(\omega)$ ,  $m = 0, 1, \dots$ , and subsequent integration one obtains a set of coupled equations for the coefficients  $a_m$ . For  $m = 0$  we obtain

$$- \frac{\omega_0 g \frac{P}{P_L} C_{00}}{Q \left( 1 + \frac{P}{P_L} \right)} a_0 (1 + e^{-2j\phi_0}) = j \Omega a_0 \tag{6.10}$$

where

$$C_{00} \equiv \int_{-\infty}^{\infty} u_0^2(\omega) \left( 1 - \frac{\omega^2}{\omega_L^2} \right) d\omega = 1 - \frac{1}{2} \frac{\omega_P^2}{\omega_L^2} \tag{6.11}$$

and  $\phi_0$  is the phase angle of  $a_0$ , i.e. the phase difference between the 0-th order component of the initial perturbation  $a_0 u_0(\omega)$  and the steady state. Note that  $C_{00} > 0$  even though

(6.11) seems to imply the possibility of negative values. We recall, however, that we have expanded a Lorentzian, an approximation valid only when the pulse bandwidth  $\omega_p$  is small compared with  $\omega_L$ . If the expansion had not been made, (6.11) would be positive definite.

Equation (6.10) is interpreted by a stability circle similar to the one discussed by Kurokawa when treating stability of injection locking of a single oscillator, Figure 9. For an arbitrary initial phase  $\phi_0$ , the frequency deviation and rate of decay are as shown in the figure. For no initial phase is growth observed. Suppose the initial phase of the perturbation  $\phi_0 > 0$  as shown in Figure 9. Then  $\text{Re } \Omega_0 > 0$  and the frequencies of the perturbations are greater than the frequencies of the steady state oscillation.  $\phi$  grows at the same rate for all modes and hence the circle is described with increasing time as shown.  $\phi$  varies as the circle is traversed. The amplitude of  $\delta V(\omega)$  decays at the rate  $\text{Im } \Omega$  which is always positive. The perturbation has relaxed when the origin is reached. If the initial phase  $\phi_0 = \pi/2$ ,  $\text{Im}(\Omega) = 0$  and no growth or decay occurs, i.e. there is no restoring force for a perturbation of this kind. A quadrature perturbation corresponds to a phase perturbation of the carrier frequency. Hence, the mode locked pulses have no carrier phase stabilization, just like a free running van der Pol oscillator[11].

Next consider the equations obtained for the perturbation amplitudes  $a_1$  and  $a_2$ . The equations for  $m > 2$  are all given by (6.8) with  $n = 0$  because the integral

$$C_{m0} \equiv \int u_m(\omega) u_0(\omega) \left( 1 - \frac{\omega^2}{\omega_L^2} - j \frac{\omega}{\omega_L} \right) d\omega$$

vanishes for all  $m \neq 0, 1, 2$ . Hence decay is predicted for all perturbations with  $m > 2$ . We have for  $m = 1$  and  $2$ :

$$-\frac{\omega_0}{2Q} (E_m - E_0) a_m - \frac{\omega_0 g \frac{P}{P_L}}{Q \left( 1 + \frac{P}{P_L} \right)} C_{m0} \operatorname{Re} a_0 = j\Omega a_m \quad (6.12)$$

where

$$C_{10} = -j \int u_0 u_1 \frac{\omega}{\omega_L} d\omega$$

and

$$C_{20} = - \int u_0 u_2 \left( 1 - \frac{\omega^2}{\omega_L^2} \right) d\omega .$$

This equation shows that  $\operatorname{Re} a_0$  acts as a source of these perturbations. In fact, a proper interpretation of (6.12) is obtained only after one recalls that  $j\Omega$  is equivalent to a time derivative in the spirit of the present analysis (and Kurokawa's stability analysis) which deals with the time evolution of an instantaneous amplitude and frequency.

Since the natural "frequencies" of the system of (6.12) are decaying exponentials, (6.12) predicts solely that the lowest order perturbation  $m = 0$  produces  $m = 1$  and  $m = 2$  pertur-

bations while it decays according to (6.10). These excitations of  $m = 1$  and  $m = 2$  in turn vanish along with the decay of the  $m = 0$  perturbation.



## VII. Conclusions

The analysis of forced mode locking as a problem of injection locking led naturally to approximations which would have been less evident in a different approach. In particular, the expansion of the laser medium susceptance in terms of frequency deviation introduced, in the time domain, first and second derivatives as a description of pulse distortion by the laser medium. This approximation reduced every forced mode locking analysis to a Schroedinger equation. Detuning of the mode locking drive introduces first derivatives which can be removed by writing the function  $v(t)$  as a product of an exponential multiplying factor and another time function. The displacement of the mode locking crystal is represented simply as a shaping and a repetition of the "potential well". The inhomogeneously broadened mode locked laser could be treated by this new approach. The stability analysis of the mode locked solution reduced to a problem in essence treated by Kurokawa.

It is believed that the potential of the present analysis has been hardly tapped and that many other issues of interest, both in forced mode locking and saturable absorber mode locking, will be analyzable using this new approach.

### Acknowledgment

The author is grateful to Mr. Wallace Wong, who obtained the computer solution of Figures 5, 6, and 7. He also acknowledges the many useful discussions with Mr. C. Ausschnitt.

Figure Captions

1. Equivalent circuit for single mode, injection locked oscillator.
2. The balancing of admittance discrepancy by injected currents produced by mode locking modulation.
3. The force-field-potential as a function of "time".
4. The normalized amplitude versus normalized frequency of the lowest order supermode for an inhomogeneously broadened laser.
5. Range of normalized gain and normalized mode locking modulation within which steady state mode locking solutions with single peak are found.
6. Amplitude at line center as function of normalized modulation.
7. "Deep" modulation and the quantum mechanical wave function analog.
8. The equivalent "well" for mode locking element in cavity center and square wave modulation.
9. The stability circle.

### Appendix I

In this Appendix we derive the circuit equations used in the body of the paper for the mode locking analysis. We assume an open cavity formed by curved mirrors in free space, portions of which are filled by the laser medium and the mode locking element. The electromagnetic field in the cavity obeys Maxwell's equations

$$\nabla \times \bar{E} = -\mu_0 \frac{\partial \bar{H}}{\partial t} \quad (I.1)$$

$$\nabla \times \bar{H} = \epsilon_0 \frac{\partial \bar{E}}{\partial t} + \bar{J} \quad (I.2)$$

In these equations  $\bar{J}$  represents the perturbation of the cavity modes by the losses, the laser medium, and the mode locking element. We expand the electromagnetic field in terms of the cavity modes with normalized field patterns  $\bar{e}_k(r)$  and  $\bar{h}_k(r)$  for the electric and magnetic field respectively. These mode patterns are related by

$$\nabla \times \bar{e}_k = \beta_k \bar{h}(\bar{r}) \quad (I.3)$$

$$\nabla \times \bar{h}_k = \beta_k \bar{e}(\bar{r}) \quad (I.4)$$

where  $\beta_k$  is related to the resonant frequency  $\omega_{k0}$  of the cavity.

$$\beta_k = \frac{\omega_{ko}}{c} \quad (I.5)$$

These field patterns are divergence free.

$$\nabla \cdot \bar{e}_k = 0 \quad (I.6)$$

$$\nabla \cdot \bar{h}_k = 0 \quad (I.7)$$

In general, an expansion in modes having divergence is also necessary[12]. However, the effect of these modes is negligible in optical cavities. We shall omit contributions due to such modes.

The field patterns are orthogonal and may be normalized.

$$\int \bar{e}_k \cdot \bar{e}_l^* dv = \int \bar{h}_k \cdot \bar{h}_l^* dv = N \delta_{kl} \quad (I.8)$$

Here  $N$  is a normalization constant whose choice is dictated by convenience. To be specific, one may consider a Gaussian mode whose field pattern is proportional to

$$\bar{e}_k(\bar{r}) \propto \frac{2}{\sqrt{\pi L}} \frac{\sqrt{N}}{w(z)} \sin \beta_k z e^{-r^2/w^2} \quad (I.9)$$

where  $L$  is the spacing between the mirrors and  $w$  is the beam diameter which is the well known function of position  $z$  and radii of curvature of the mirrors[13]. One may assume that at the mirrors the boundary condition is met that the tangential electric field vanishes. The field is approximately transverse

to the direction of propagation, the polarization vector lies in the surface of constant phase.

Use of the mode patterns effects a separation of the time dependence from the spatial dependence. One may write

$$\bar{\mathbf{E}}(\bar{\mathbf{r}}, t) = \sum_k \underline{v}_k(t) \bar{\mathbf{e}}_k(\bar{\mathbf{r}}) e^{j\omega_0 t} + \text{C.C.} \quad (\text{I.10})$$

$$\bar{\mathbf{H}}(\bar{\mathbf{r}}, t) = \sum_k \underline{i}_k(t) \bar{\mathbf{h}}_k(\bar{\mathbf{r}}) e^{j\omega_0 t} + \text{C.C.} \quad (\text{I.11})$$

where we display only the positive frequency parts and extricate explicitly the fast time dependence  $\exp j\omega_0 t$  corresponding to the center frequency of the laser line. We indicate all frequency components from which the fast time dependence has been extracted by a bar under the letter. When these expansions are introduced into Maxwell's equations and the orthogonality conditions (I.8) are utilized, one obtains differential equations in time for the amplitudes  $\underline{i}_k(t)$  and  $\underline{v}_k(t)$ , the equivalent currents and voltages.

$$\underline{v}_k = -L_k \left( j\omega_0 + \frac{d}{dt} \right) \underline{i}_k \quad (\text{I.12})$$

$$\underline{i}_k = \left\{ C_k \left( j\omega_0 + \frac{d}{dt} \right) \underline{v}_k + \frac{1}{\beta_k N} \int \bar{\mathbf{J}} \cdot \bar{\mathbf{e}}_k^* dv \right\} \quad (\text{I.13})$$

The equivalent capacitance and inductances of (I.12) and (I.13)

are given by

$$C_k = \frac{\epsilon_o}{\beta_k} = \frac{1}{\omega_{ko}} \sqrt{\frac{\epsilon_o}{\mu_o}}$$

$$L_k = \frac{\mu_o}{\beta_k} = \frac{1}{\omega_{ko}} \sqrt{\frac{\mu_o}{\epsilon_o}} \quad (\text{I.14})$$

The resonance frequencies of an optical cavity are evenly spaced, so that

$$\omega_{ko} = \omega_o + k\Delta\omega \quad (\text{I.15})$$

where  $\omega_o$  is the frequency of the mode nearest laser-line center and the mode index  $k$  assumes positive and negative values.

If mode locking is achieved, the frequencies  $\omega_k$  of the Fourier components of the field will be evenly spaced with the frequency separation  $\omega_M$ , where  $\omega_M$  is the frequency of modulation of the mode locking element. Because of the resonant nature of (I.12) and (I.13), the time dependence of the  $k$ -th cavity mode will be essentially  $\exp j \omega_k t$  where  $\omega_k$  is the frequency of the spectral component nearest the resonance frequency  $\omega_{ko}$  of the cavity. This implies, on one hand, that  $\omega_M$  must be near  $\Delta\omega$  and that

$$\omega_k = k \omega_M + \omega_o \quad (\text{I.16})$$

where  $\omega_0$  is the frequency of oscillation of the mode nearest to laser line center. In fact, the  $\omega_0$ 's in (I.15) and (I.16) need not be identical; but in the case of cavity modes spaced closely compared to the laser line-width one will always find a mode near line center that oscillates essentially at its resonance frequency. The equation of the amplitude of the  $k$ -th cavity mode, whose amplitude has the time dependence  $\exp j \omega_k t$  as explained above is:

$$j B_C(\omega_k) \underline{v}_k + \frac{1}{\beta_k N} \int \underline{\bar{J}} \cdot \bar{e}_k^* dv \Big|_k = 0 \quad (\text{I.17})$$

where the "susceptance" of the  $k$ -th mode is

$$B_C(\omega_k) = (\omega_0 + \omega_k) C_k - \frac{1}{(\omega_0 + \omega_k) L_k} \approx 2 \frac{Q}{\omega_0} k(\omega_M - \Delta\omega) G_C$$

$$\text{where } Q \equiv \frac{\omega_{k0} C_k}{G_C} \approx \frac{\omega_0 C}{G_C} \quad (\text{I.18})$$

with  $G_C$  to be defined later, and  $\omega_{k0}$  and  $C_k$  are approximated as independent of mode number  $k$ . Here we have denoted the Fourier component of the last term in (I.17) at frequency  $\omega_k$  by a vertical bar followed by the subscript  $k$ . This is the driving term for the  $k$ -th cavity mode which contains in addition to the injected signal due to the mode locking modulation a contribution of the cavity loss and the laser medium gain. We assume that the



positive frequency part of  $\bar{J}$ , with  $e^{j\omega_0 t}$  omitted,  $\bar{J}$ , may be written in the form

$$\bar{J}(\bar{r}, t) = [\sigma_C(\bar{r}) + j\omega_0 \epsilon_0 \chi_L(\bar{r}) + \sigma_M(\bar{r}, t)] \bar{E}(\bar{r}, t). \quad (I.19)$$

The first term is an equivalent conductivity representing the cavity losses. The second term includes the complex polarizability  $\chi_L$  of the laser medium. The last term is the modulated conductivity produced by the mode locking element, under the assumption of resistive modulation. A modulation of a dielectric constant can be treated by replacement of the conductivity by an imaginary quantity. In (I.19) it has been assumed that the cavity loss and the laser medium susceptibility are time independent and hence produce no modulation sidebands of the electric field. The instantaneous variation in laser gain as produced by a passage of a mode locked pulse have been disregarded. This means that the assumption has been made that the laser medium relaxation time  $T_1$  is very long and hence the laser medium responds only to the time independent power of the mode locked pulse train. The  $k$ -th Fourier component of the driving term of the  $k$ -th mode in (I.16) assumes then the following form

$$\left. \frac{1}{\beta_k N} \int \bar{J} \cdot \bar{e}_k(\bar{r}) dv \right|_k = [G_C + Y_L] \bar{V}_k + G_C \sum_l m_{kl}(t) \frac{\bar{V}(t)}{l} \Big|_{\substack{k\text{-th Fourier} \\ \text{component}}}$$

(I.20)

where the various coefficients have been defined

$$G_C \approx \frac{1}{\beta_{0N}} \int \sigma_C(\bar{r}) \bar{e}_k \cdot \bar{e}_h^* dv \quad (I.21)$$

$$Y_L = \frac{1}{\beta_{0N}} \int \chi_L(\bar{r}) \bar{e}_k \cdot \bar{e}_k^* dv \quad (I.22)$$

$$G_C m_k(t) \approx \frac{1}{\beta_{0N}} \int \sigma_M(\bar{r}, t) \bar{e}_k^* \cdot \bar{e}_l dv \quad (I.23)$$

If the modelocking element is near one of the mirrors, the integral becomes  $k$ - and  $l$ - independent and one may then omit the subscripts  $k, l$ . This has been done in the first part of the text. If the laser medium and the equivalent loss are nonuniformly distributed through the cavity, then coupling is produced between the different mode patterns. This coupling leads to injection signals caused by the  $k$ -th Fourier component into modes of index  $l \neq k$ . Such injection signals excite the mode off resonance and therefore produce a negligible effect and will be disregarded. The conductance assigned to the mode locking element, on the other hand, because of its time variation, produces Fourier components at frequencies other than the frequency of the driving electric field, and hence coupling between the modes due to this conductivity  $\sigma_M$  must be included. Introducing (I.18) through (I.23) into (I.17), we finally obtain the desired relationship

$$\left\{ G_C \left[ 1 + j \frac{k\omega_M}{\omega_0} 2Q \frac{\omega_M - \Delta\omega}{\omega_M} \right] + Y_L(\omega_k) \right\} v_k$$

$$= - G_C m(t) \sum_l v_l e^{j l \omega_M t} \Big|_{k\text{-th Fourier component}} \quad (\text{I.24})$$

This is (1.10) of the text.

Next we study the effect of gain saturation and the approximations necessary to lead to manageable equations. The rate equation for the population inversion for a driving field near the resonance frequency of the medium is

$$\frac{\partial n}{\partial t} = - \frac{n - n_e}{T_1} - 2 \left| \frac{\bar{\mu} \cdot \bar{E}}{\hbar} \right|^2 T_2 n \quad (\text{I.25})$$

Here  $\mu$  is the matrix element of the laser levels. We assume that all Fourier components of the electric field lie sufficiently near the resonance of the laser medium so that all Fourier components in  $E$  may be assumed to have an identical depleting effect on the population inversion. If one assumes that the relaxation time  $T_1$  of the laser medium is long enough so that the laser medium cannot respond to the time dependent components of the mode locked laser pulses, one may write for the population inversion approximately

$$n = n_e \left\{ 1 - 2 \left\langle \left| \frac{\mu \bar{E}}{\hbar} \right|^2 \right\rangle T_1 T_2 \right\} \quad (\text{I.26})$$

where  $\langle \rangle$  indicates a time average. The time independent component of the square of the electric field may be written

$$\langle |E|^2 \rangle = \sum_k |v_k|^2 \bar{e}_k \cdot \bar{e}_k^* \quad (\text{I.27})$$

We are interested in the term, (compare (I.22)):

$$\int \chi_L \bar{e}_k \cdot \bar{e}_k^* dv \propto \int dv \bar{e}_k \cdot \bar{e}_k^* \left\{ 1 - 2 T_1 T_2 \left| \frac{\mu}{\hbar} \right|^2 \sum_l \bar{e}_l \cdot \bar{e}_l^* |v_l|^2 \right\} \quad (\text{I.28})$$

A simple evaluation is possible if the laser medium is short and positioned near one of the mirrors of the optical cavity. Using the mode pattern (I.9), one has for the second term in brackets of (I.27)

$$\int dv (\bar{e}_k \cdot \bar{e}_k^*) (\bar{e}_l \cdot \bar{e}_l^*) = \frac{3N^2}{2\pi L w^2} \frac{\theta_L}{L} \quad (\text{I.29})$$

where we have made the assumption that the propagation constant  $\beta$  is identical for all modes of interest an assumption valid if the integration is to be carried over a volume short compared to the optical cavity length and situated near one end of the cavity;  $\theta_L$  is the length of the laser medium. With this finding one may write for the integral (I.27):

$$\int \chi_L \bar{e}_k \cdot \bar{e}_k^* dv = \int \chi_L^0 \bar{e}_k \cdot \bar{e}_k^* dv \left\{ 1 - \frac{\sum |V_\ell|^2}{P_L} \right\} \quad (I.30)$$

where the saturation power  $P_L$  is defined by

$$\frac{1}{P_L} = \frac{3 N}{\pi L w^2} \left| \frac{\mu}{h} \right|^2 T_1 T_2 \quad (I.31)$$

When the medium fills the entire cavity, the integral in (I.28) is somewhat more complicated and in fact what is included by carrying out the integral is the effect of spatial hole burning, an effect not to be considered in the present study.

One may generalize (I.30) to be valid approximately also for large field intensities by replacing the factor  $1 - \sum V_n^2/P_L$  by  $1/(1 + \sum V_n^2/P_b)$ . This is the form used in the bulk of the paper.

It is convenient to normalize the "voltage" components so that their mean square amplitude gives the power in one of the

two counter travelling waves in the standing wave cavity. With the mode pattern (I.9) the peak amplitude of the electric field of a travelling wave component is

$$E_{\text{peak}} = \frac{2\sqrt{N}}{\sqrt{\pi L}} \frac{1}{w} e^{-r^2/w^2}. \quad (\text{I.32})$$

If one implies that the integral of the power density of the wave over the cross-section of the optical beam be equal to the voltage amplitude squared, one obtains the relation for the normalization constant  $N$

$$N = \pi L \sqrt{\frac{\mu_0}{\epsilon_0}}. \quad (\text{I.33})$$

This is the normalization employed in the bulk of the paper.

### References

- [1] A. J. DeMaria, W. H. Glenn, M. J. Brienza, M. E. Mack, "Picosecond Laser Pulses", Proc. IEEE, vol. 57, no. 1, Jan. 1969, pp. 2-25.
- [2] D. J. Kuizenga, A. E. Siegman, "FM and AM Mode Locking of the Homogeneous Laser - Part I: Theory", IEEE JQE, vol. QE-6, no. 11, Nov. 1970, p. 694.
- [3] O. P. McDuff, S. E. Harris, "Nonlinear Theory of the Internally Loss-Modulated Laser", IEEE JQE, vol. QE-3, no. 3, March 1967, p. 101.
- [4] K. Kurokawa, "Injection Locking of Microwave Solid-State Oscillators", Proc. IEEE, vol. 61, Oct. 1973, pp. 1386-1410.
- [5] V. S. Letokhov, "Dynamics of Generation of a Pulsed Mode Locking Laser", Soviet Physics JETP, vol. 27, no. 5, Nov. 1968, pp. 746-751. Letokhov has replaced the discrete frequency spectrum of the cavity modes by a continuum. He did not take into account the laser gain profile and hence did not get the same steady state solutions.

- [6] L. D. Landau, E. M. Lifshitz, "Nonrelativistic Theory", Quantum Mechanics, Addison Wesley, Pergamon Press, 1958.
- [7] H. Haken, M. Pauthier, "Nonlinear Theory of Multimode Action in Loss Modulated Lasers", IEEE JOE, vol. QE-4, no. 7, July 1968, pp. 454-459. They made assumptions similar to ours and obtained similar mode solutions. They did not investigate the stability of the solutions.
- [8] T. J. Nelson, "A Coupled-Mode Analysis of Mode Locking in Homogeneously Broadened Lasers", IEEE J. Quant. Elect., vol. QE-8, Feb. 1972.
- [9] D. M. Kim, S. Marathe, T. A. Rabson, "Eigenfunction Analysis of Mode-Locking Process", J. Appl. Phys., vol. 44, April 1973.
- [10] A. E. Siegman and D. J. Kuizenga, "Modulator Frequency Detuning Effects in the FM Mode-Locked Laser", IEEE J. Quan. Elect., vol. QE-6, Dec. 1970.
- [11] J. A. Mullen, "Background Noise in Nonlinear Oscillators," Proc. IRE, vol. 48, August 1960, pp. 1454-1466.



- [12] J. C. Slater, "Microwave Electronics", D. Van Nostrand Co., Inc., New York, 1950.
- [13] A. Yariv, "Introduction to Optical Electronics", Holt Rinehart Winston, 1971.

Figure 1.

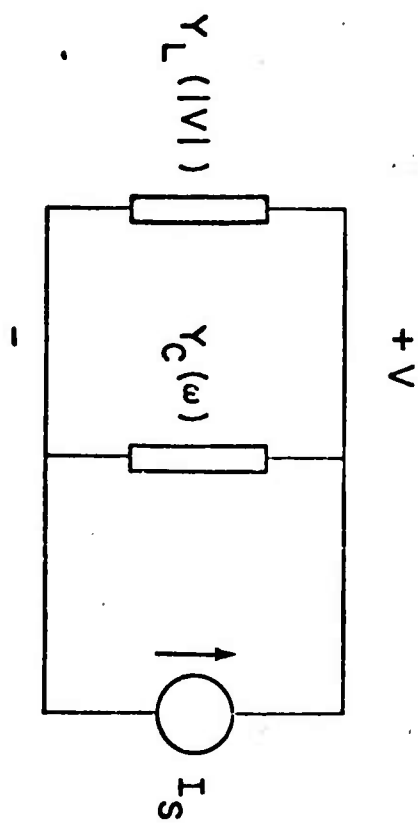


Figure 2.

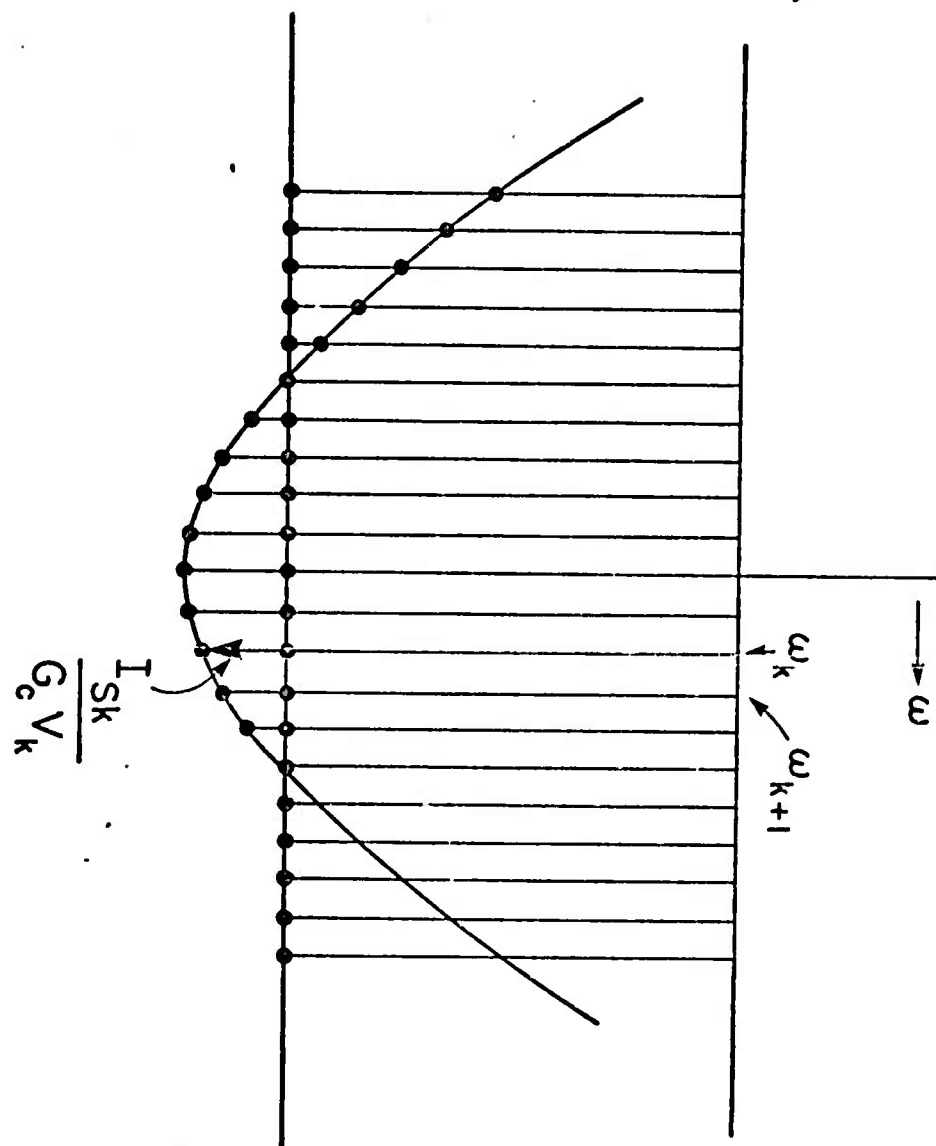
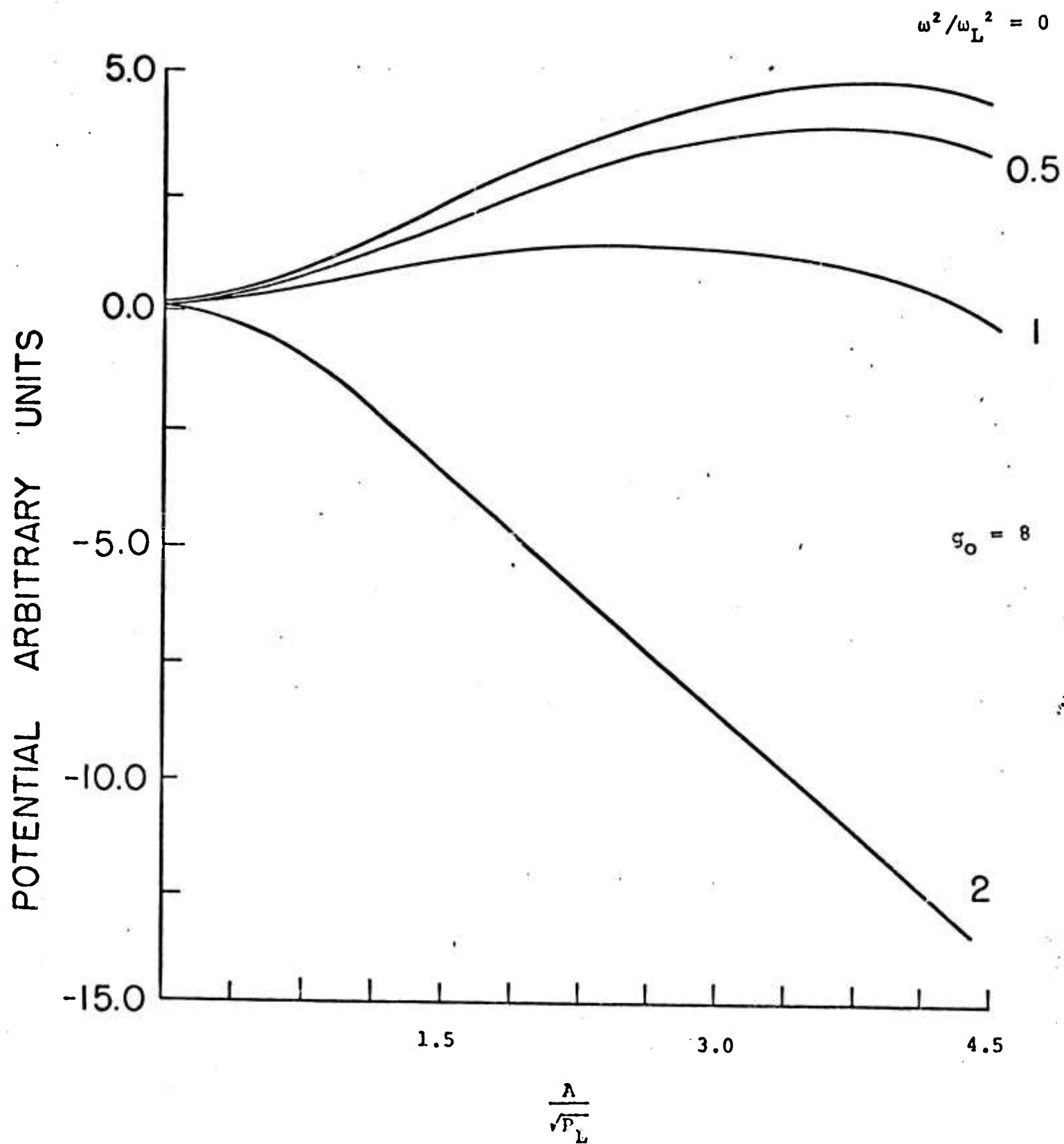
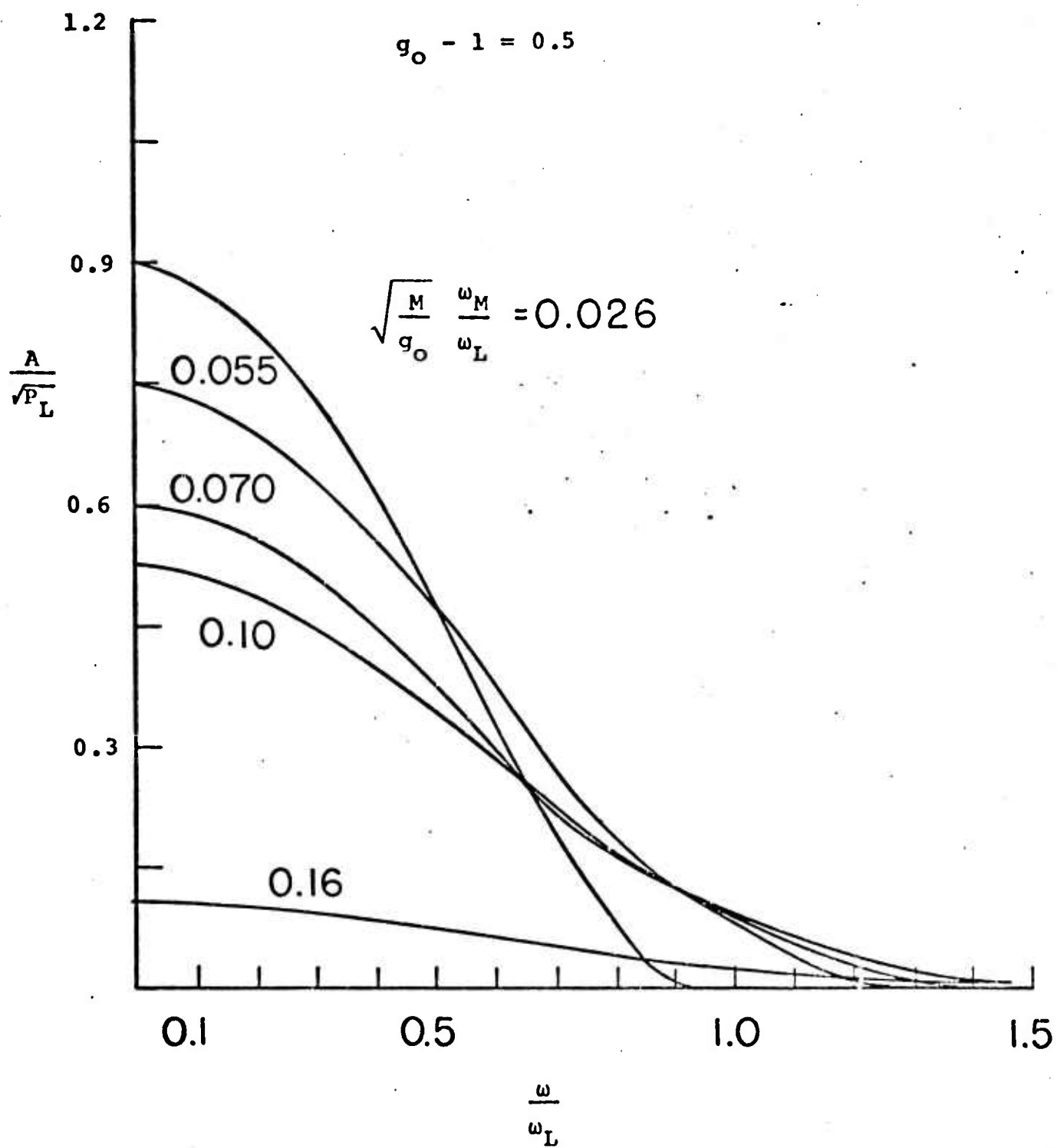


Figure 3.





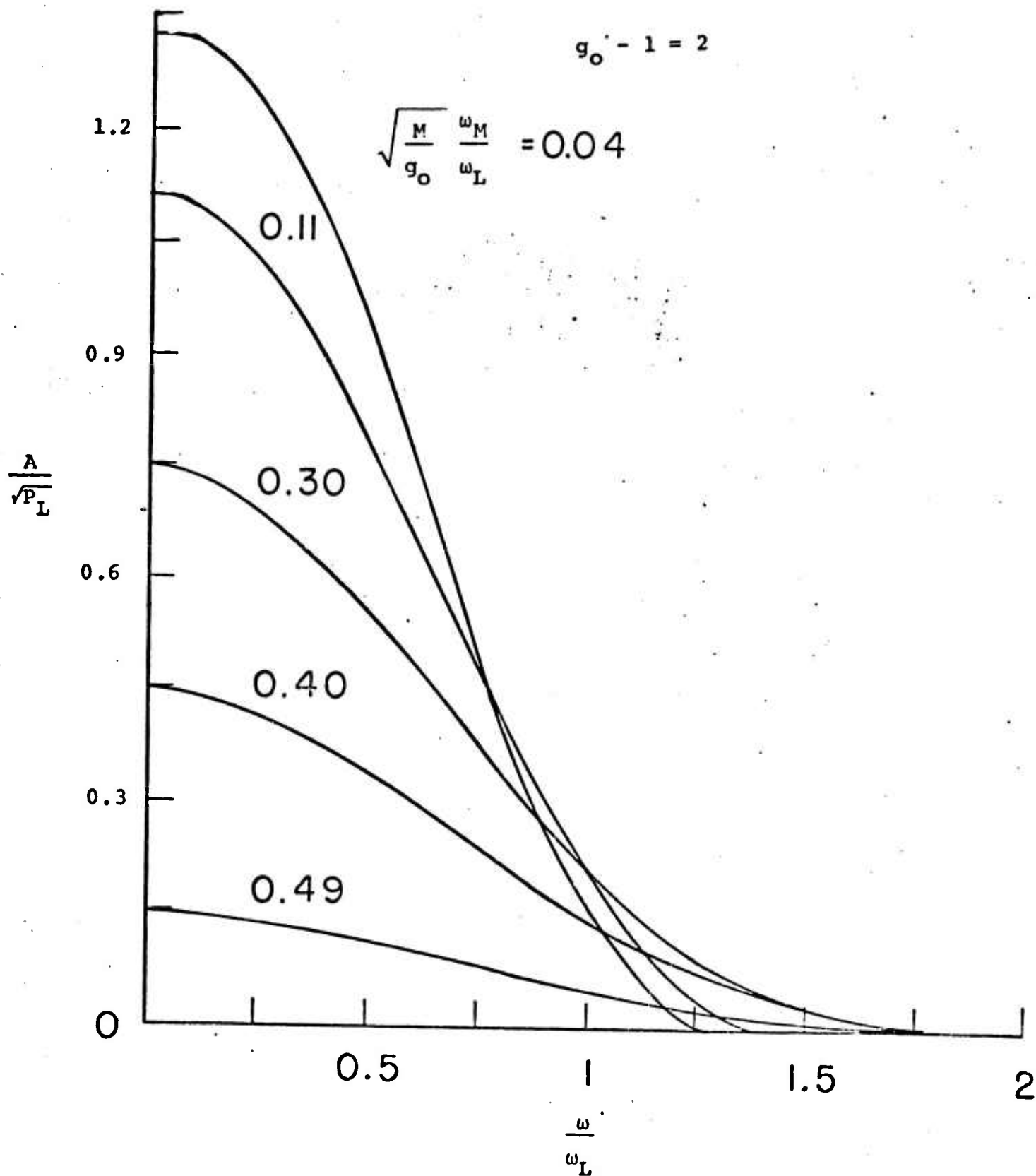


Figure 5.

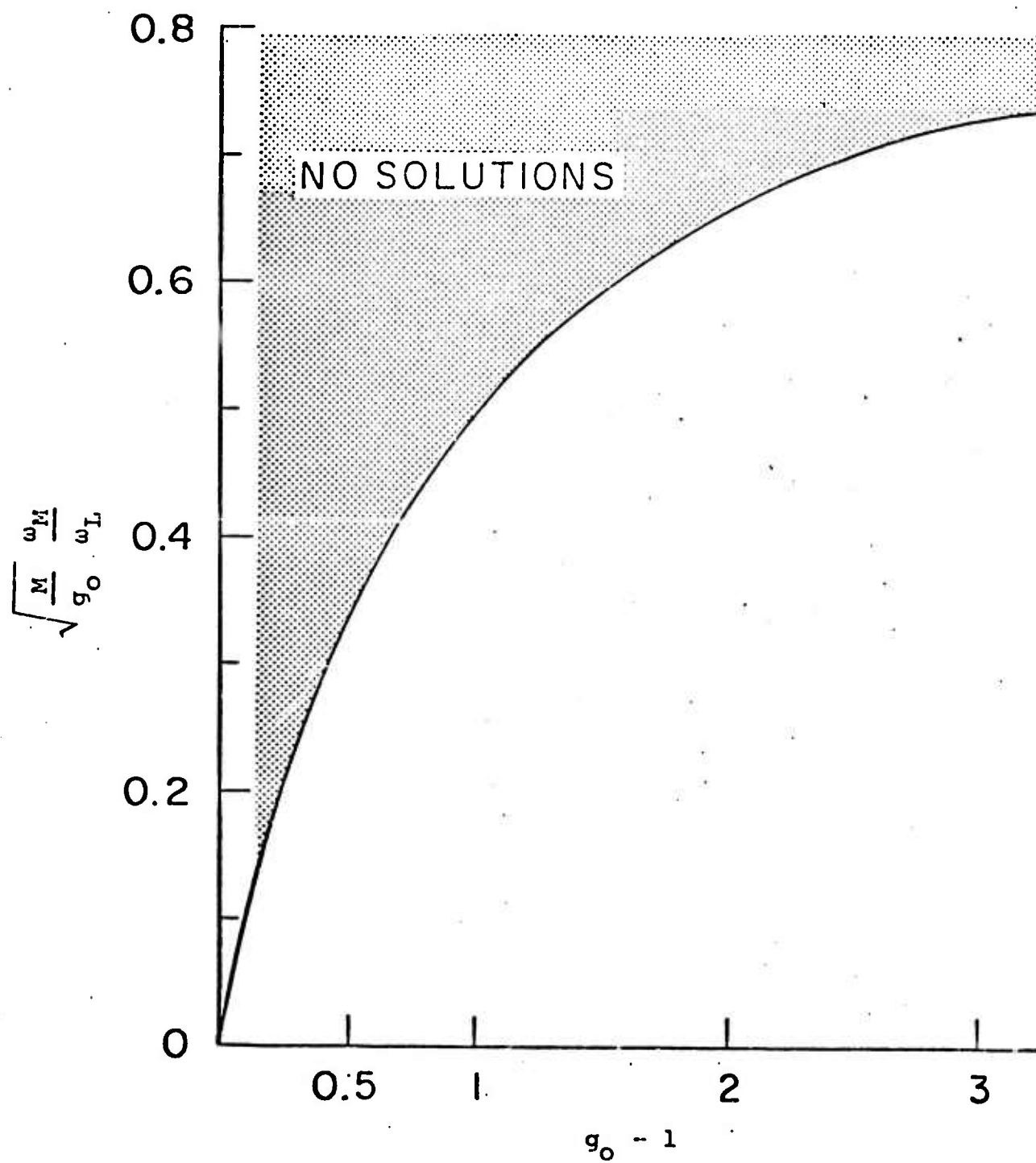


Figure 6.

59

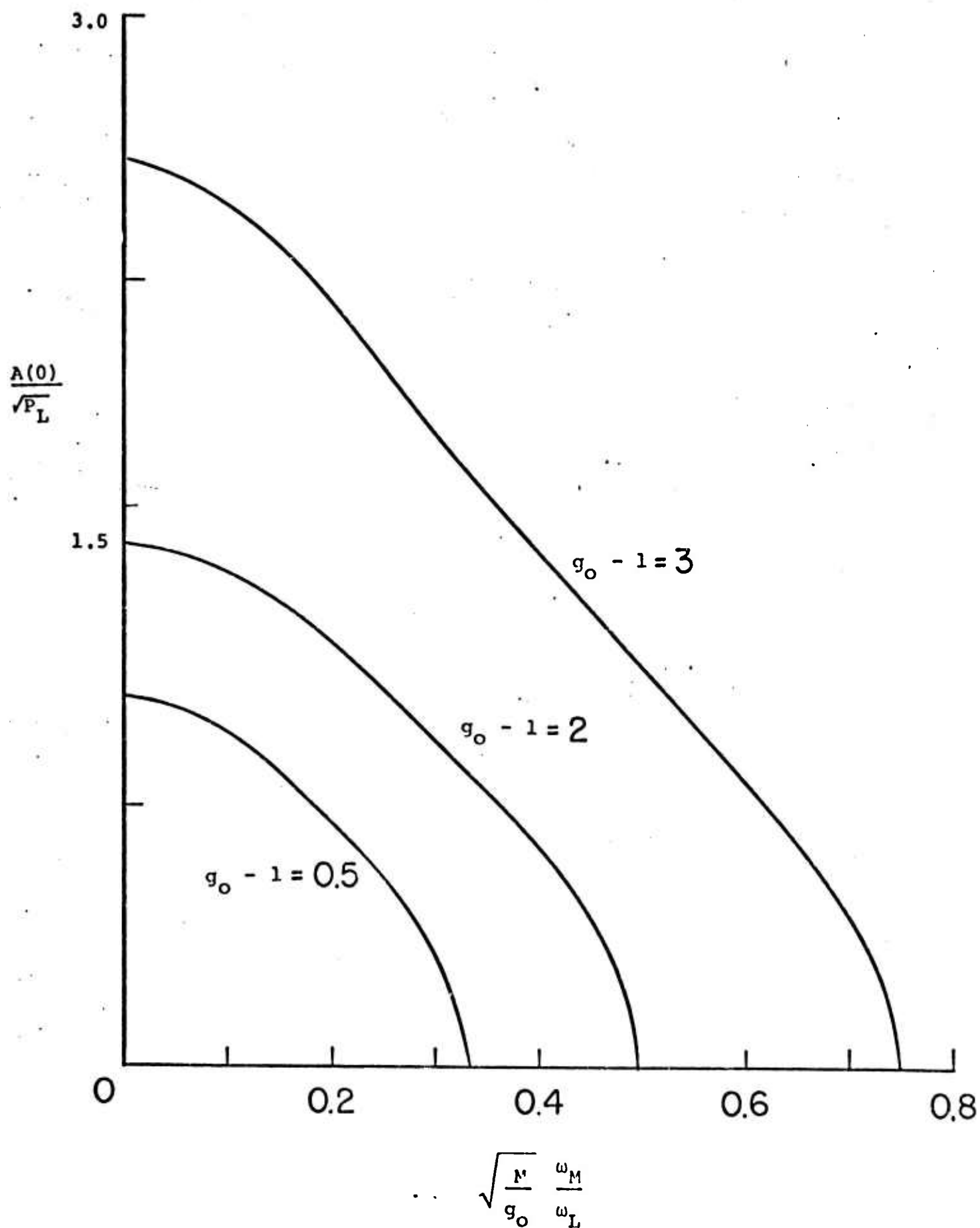




Figure 7.

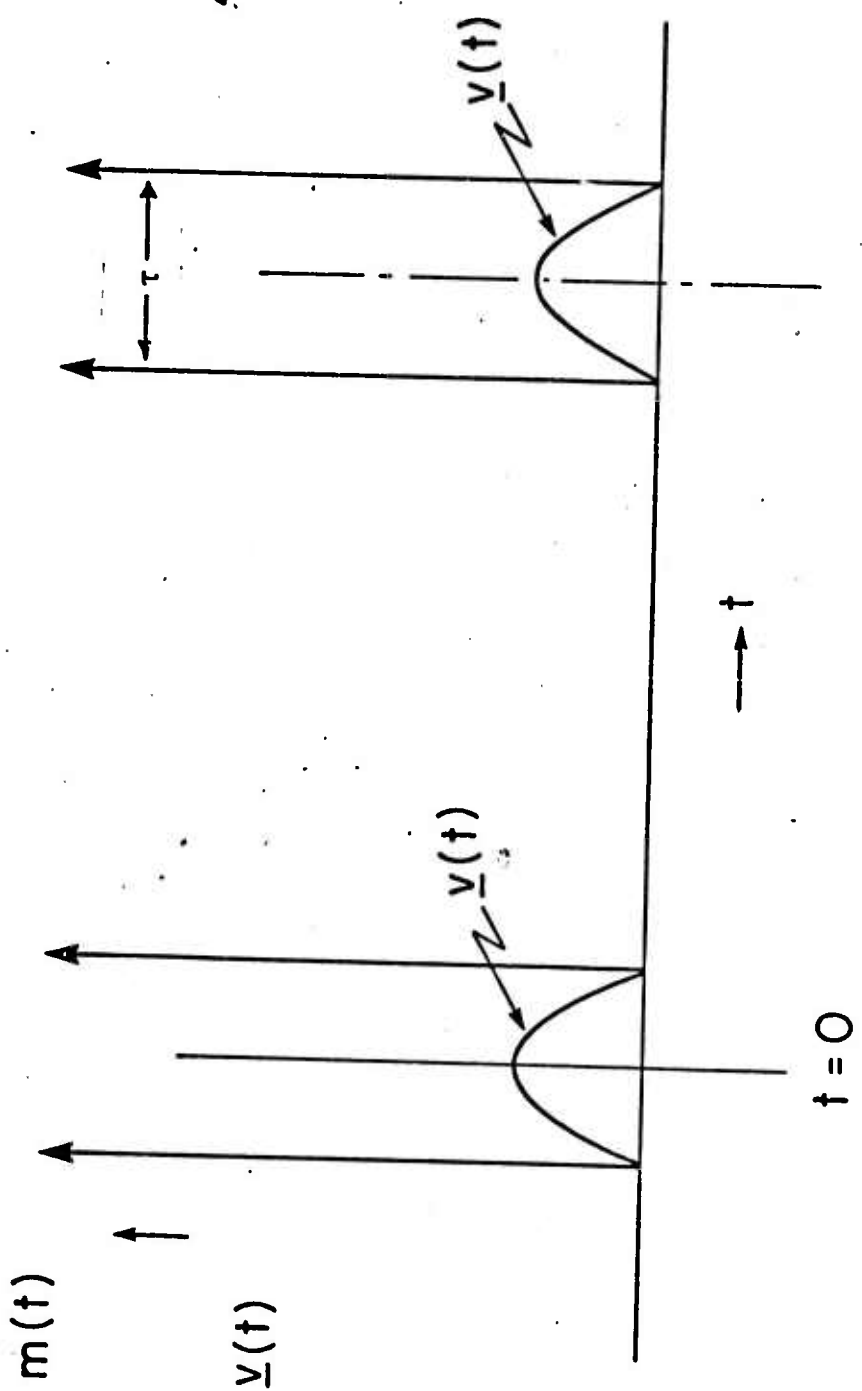


Figure 8.

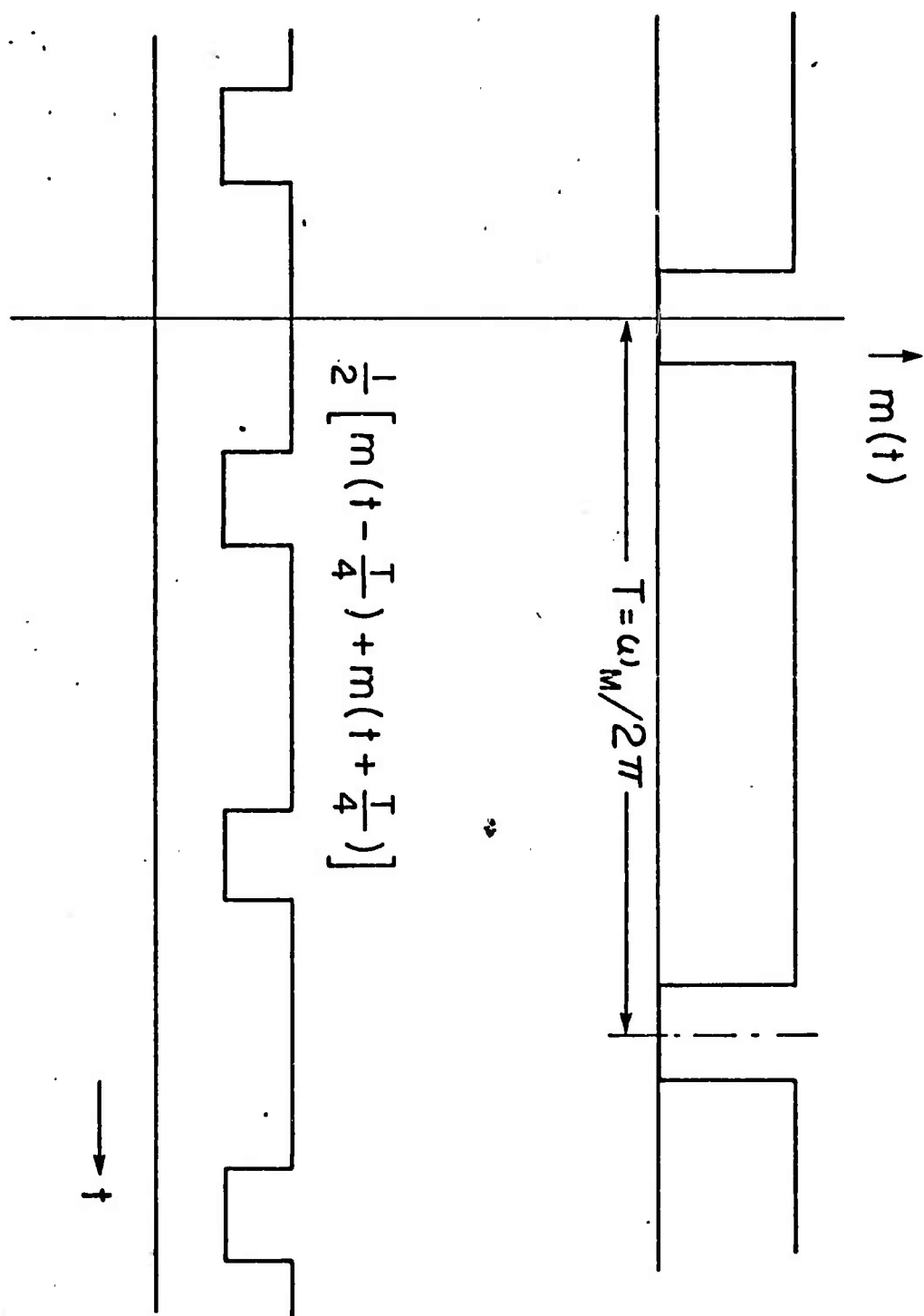
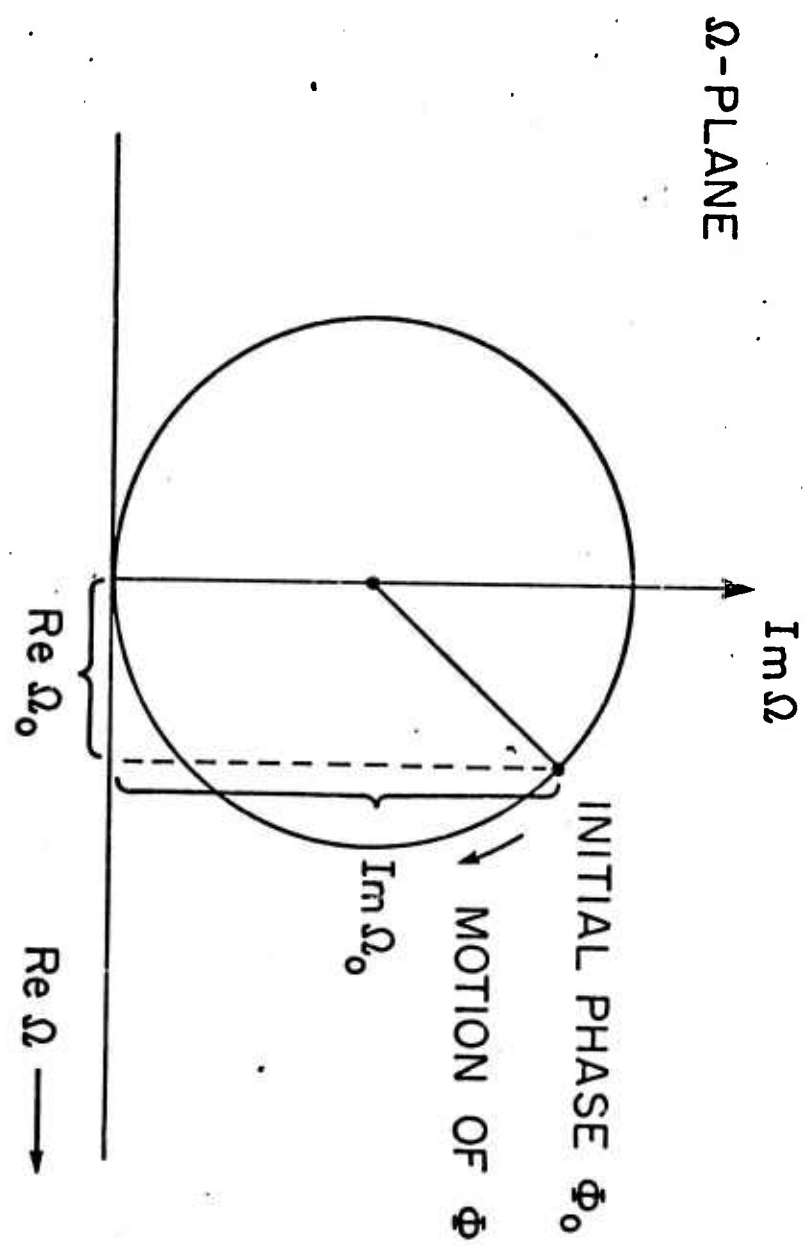


Figure 9.



## APPENDIX V

Preprint: to be submitted for publication

H. A. Haus, "Mode Locking with a Fast Saturable Absorber"

68

MODE LOCKING WITH A FAST SATURABLE ABSORBER\*

H. A. Haus\*\*

Abstract

A closed form solution is obtained for mode locking of a laser by a saturable absorber with instantaneous response. The laser medium gain is assumed time independent. The solution, as a function of time, is a hyperbolic secant.

---

\* Work supported by US Army Research Office - Durham (Contract DAHC04-72-C-0044).

\*\* Electrical Engineering Department & Research Laboratory of Electronics, Massachusetts Institute of Technology, Cambridge, Mass. 02139.

## I. Introduction

In another publication, we have developed a theory of forced mode locking in the frequency domain (see appendix IV). With some modifications of this mode locking theory, it is possible to obtain what we believe is the first closed-form solution for saturable absorber mode locking.

As in the case of forced mode locking, we treat mode locking by a saturable absorber as a form of injection locking. This means that the admittance mismatch of the resonant circuit representing a cavity mode is balanced by the injection locking current produced through interaction of the equivalent cavity voltage (i.e. electric field amplitude) with the saturable absorber.

In equation form:

$$[Y_{Ck}(\omega_k) + Y_L(\omega_k)] V_k = I_{Sk}. \quad (1.1)$$

Here  $Y_{Ck}$  is the equivalent admittance of the  $k$ -th axial cavity mode and  $Y_L$  is the equivalent admittance of the laser medium. The reader is referred to appendix IV for details of the derivation. The following approximations are made:

(a) The mode susceptance is expressed as a linear function of frequency deviation from the mode resonance frequency  $\omega_{k0}$  and the equivalent conductance is assumed mode independent

$$Y_C(\omega_k) = G_C \left[ 1 + 2j \frac{Q}{\omega_0} (\omega_k - \omega_{k0}) \right] \quad (1.2)$$

(b) The laser medium equivalent admittance has a Lorentzian shape that is approximated by an expansion in frequency

$$Y_L(\omega_k) \approx -G_C g \left[ 1 - j \frac{\omega_k - \omega_0}{\omega_L} - \frac{(\omega_k - \omega_0)^2}{\omega_L} \right] \quad (1.3)$$

Here,  $g$  is power dependent, where  $P$  is equal to the sum of the counter traveling powers of the standing waves of each axial mode.

$$g = \frac{g_0}{1 + \frac{P}{P_L}} \quad (1.4)$$

The saturation expression is approximately independent of frequency if the frequency spectrum of the pulse is narrow compared with the linewidth.

(c) All Fourier components of the amplitude of the  $k$ -th axial mode other than the one near the cavity resonance are neglected (high  $Q$  approximation).

(d) One assumes that mode locking is successful, i.e. that a solution of periodic pulses does exist, so that all Fourier components are evenly spaced at separations  $\omega_M$ . The frequency of the  $k$ -th axial mode amplitude is

$$\omega_k = k \omega_M + \omega_0 \quad (1.5)$$

where  $\omega_0$  is the frequency of the mode nearest medium line center (set approximately at line center, an assumption legitimate if the mode spectrum is dense).

(e) The injection current  $I_{Sk}$  in (1.1) is assumed to be produced by modulation products of the equivalent mode voltages (electric fields). The loss element is assumed to interact equally with all modes (i.e. the element is thin and near one of the laser cavity mirrors).

$$I_{Sk} = - G_C m(t) \sum_l V_l e^{jl\omega_M t} \quad (1.6)$$

The separation of the resonance frequencies  $\omega_{ko}$  of the axial modes is constant,  $\Delta\omega$ , and thus

$$\omega_{ko} = k \Delta\omega + \omega_0. \quad (1.7)$$

(1.5) and (1.7) imply that the central mode,  $k = 0$ , oscillates at resonance, an assumption justified by the fact that we obtain a solution.

Introducing (1.2), (1.3), (1.5), (1.6), and (1.7) into (1.1) we obtain

$$\left\{ 1 + jk\omega_M \left( \frac{2Q}{\omega_0} \frac{\omega_M - \Delta\omega}{\omega_M} + g \frac{1}{\omega_L} \right) - g \left[ 1 - \frac{(k \omega_M)^2}{\omega_L^2} \right] \right\} V_k$$

$$= - m(t) \sum_l V_l e^{jl\omega_M t} \quad (1.8)$$

k-th Fourier component



The right hand side of (1.8) is more conveniently expressed in the time domain, as  $-m(t) v(t)$  where

$$v(t) = \sum_l V_l e^{j l \omega_M t} \quad (1.9)$$

is the time dependent amplitude of the standing wave electric field near the mirror (next to which the saturable absorber is situated). One may look, therefore, for simplification of (1.8) by expressing the entire equation in the time domain. Multiplying the left hand side by  $\exp j k \omega_M t$ , adding over all  $k$  and noting that multiplication by  $(j k \omega_M)^n$  is  $d^n/dt^n$  in the time domain, one has

$$\left[ 1 + (\delta + g) \frac{1}{\omega_L} \frac{d}{dt} - g \left( 1 + \frac{1}{\omega_L^2} \frac{d^2}{dt^2} \right) \right] v(t) = -m(t) v(t) \quad (1.10)$$

where

$$\delta \equiv 2Q \frac{\omega_M - \Delta\omega}{\omega_O} \frac{\omega_L}{\omega_M} \quad (1.11)$$

The equation describes the change wrought on a pulse of the electric field by the action of the cavity and the laser medium and sets this change equal to the change caused on the pulse by the time dependent element as expressed by  $m(t)$ . The term  $1 \times v(t)$  is proportional to the distortion-free decrease of the pulse caused by the cavity loss. The laser gain produces a change proportional to

$$g \left( 1 + \frac{1}{\omega_L^2} \frac{d^2}{dt^2} \right) v.$$

If  $v$  is a single pulse with two inflection points, the second derivative is a pulse with three extrema. Remember that  $d^2/dt^2$  is the Fourier transform operator of  $-\omega^2$ . Hence this contribution expresses the deficiency of gain at larger frequency deviations from line center as compared to the gain at the center frequency. The pulse with the three extrema subtracts at the center of the original pulse ( $t \rightarrow 0, \omega \rightarrow \infty$ ) and adds on the wings ( $|t| \rightarrow \infty, \omega \rightarrow 0$ ). The pulse passing through the medium is amplified and broadened (in time).

On the right hand side appears the (negative) change produced by the time varying element, in our case the saturable absorber. This element has to compensate for the shape change produced by the laser medium.

For the purpose of relating to the derivation in the next section, note that  $m(t)$  as produced by a saturable absorber may be written as  $Q/Q_A(t)$  where  $Q$  is the cavity quality factor in the absence of the absorber and  $1/Q_A(t)$  is the time dependent inverse  $Q$  of the saturable absorber.

## II. The Saturable Absorber

The rate equation for the population difference  $n$  between the lower and the upper levels of the saturable absorber is

$$\frac{\partial n}{\partial t} = - \frac{n - n_e}{T_A} - 2 \sigma_A \frac{|v(t)|^2}{\hbar \omega_0 A} n. \quad (2.1)$$

$v(t)$  is so normalized that  $|v(t)|^2$  gives the sum of the powers in the two counter traveling waves in the cavity added over all axial modes. Here  $T_A$  is the relaxation time of the absorbing medium,  $n_e$  is the equilibrium population difference,  $\sigma_A$  is the optical cross-section of the absorbing particles and  $A$  is the cross-section of the laser mode. If the thickness of the absorbing medium is  $\theta_A$  and the length of the cavity is  $L$ , one may define a  $Q$  associated with the absorbing medium.

$$\frac{\omega_0}{Q_A} = \frac{2 \sigma_A n_c \theta_A}{L} \quad (2.2)$$

where  $\omega_0$ , the resonance frequency of a cavity mode, is set equal to the laser line center frequency. This  $Q$  is a function of intensity and is obtained from (2.1) and (2.2) as a solution of the differential equation. If the relaxation time  $T_A$  of the absorber is fast compared with the rate of change of the intensity,

we may assume that the population difference is an instantaneous function of intensity, and obtain an approximate expression for the instantaneous  $Q$  of the saturable absorber

$$\frac{1}{Q_A} = \frac{c \theta_A^2 \sigma_A n_e}{\omega_O L} \left[ 1 - \frac{|v(t)|^2}{P_A} \right] \equiv \frac{1}{Q_A^0} \left[ 1 - \frac{|v(t)|^2}{P_A} \right] \quad (2.3)$$

where we have defined the saturation power for the absorber by

$$P_A = \frac{\hbar \omega_O A}{2 \sigma_A T_A} \quad (2.4)$$

The time-independent part of the  $Q$  of the absorber may be incorporated in the cavity loss. Thus, for the fast absorber, we obtain the differential equation

$$\left[ 1 + (g + \delta) \frac{1}{\omega_L} \frac{d}{dt} + g \left( 1 + \frac{1}{\omega_L^2} \frac{d^2}{dt^2} \right) \right] v = \frac{Q}{Q_A^0} \frac{|v(t)|^2}{P_A} v \quad (2.5)$$

We shall now look for solutions of this equation corresponding to mode locked pulses. Remember that the frequency  $\omega_M$  is an adjustable parameter, to be determined from the character of the problem. It will become clear that no periodic solutions exist when  $g + \delta \neq 0$  and thus we may state at the outset that the pulses must pick their repetition period so that  $g + \delta = 0$ . The remaining equation

$$\left[ 1 - g \left( 1 + \frac{1}{\omega_L^2} \frac{d^2}{dt^2} \right) \right] v - \frac{Q}{Q_a} \frac{|v|^2}{P_A} v = 0 \quad (2.6)$$

can be recognized as the equation of motion of a particle of displacement  $v(t)$  in a potential well

$$- \frac{1}{2} (1 - g) v^2 + \frac{1}{4} \frac{Q}{Q_a} \frac{v^4}{P_A} \quad (2.7)$$

If the particle is launched at the well height 0, at

$$v_0^2 = 2 \frac{Q_a}{Q} P_A (1 - g) \quad (2.8)$$

with zero velocity it moves to the origin and stops there. This solution is symmetric in time. A pulse like solution for the motion of the particle is then

$$v(t) = \frac{v_0}{\cosh \frac{t}{\tau_p}} \quad (2.9)$$

where

$$\frac{Q}{Q_a} \frac{v_0^2}{P_A} = \frac{2g}{\omega_L^2 \tau_p^2} \quad (2.10)$$

and

$$1 - g = \frac{g}{\omega_L^2 \tau_p^2} \quad (2.11)$$

as can be ascertained by substitution of (2.9) in (2.6).

This solution is an isolated pulse. A succession of periodic pulses, of any desired period  $2\pi/\omega_L \sqrt{2(1-g)} < T_R < \infty$  is obtained by launching the particle at a lower height. If  $\tau_p \ll T_R = 2\pi/\omega_M$  then the single pulse is an excellent approximation to one period of the periodic pulse train. Well mode locked pulses with good time separation are of this character. Since

$$\int \frac{dt}{\cosh^2 \left( \frac{t}{\tau_p} \right)} = 2\tau_p,$$

the energy in the pulse is given by  $2\tau_p v_o^2$ . The power  $P$  of the laser is then  $P = 2\tau_p v_o^2/T_R$ . Introducing this expression into (2.10), one obtains an equation between  $P$  and  $\tau_p$

$$\kappa \frac{P}{P_L} = \frac{g}{\omega_L \tau_p} \quad (2.12)$$

where we have defined the coefficient

$$\kappa \equiv \frac{Q}{4Q_A} \frac{P_L}{P_A} \omega_L T_R \quad (2.13)$$

(2.11) and (2.12) supplemented by the dependence of the negative conductance  $g$  upon power  $P$ , (1.4)

$$g = \frac{g_o}{1 + \frac{P}{P_L}}$$

yield three equations for the three unknowns  $P$ ,  $g$ , and the pulse width  $\tau_p$ .

From (2.11), we note that  $g$  is less than unity. This means that the laser is below threshold with respect to the linear loss (loss in absence of laser power). The laser oscillates because the bleaching of the absorber reduces the loss below the linear loss. The equivalent injection locking voltages have to be equal to the difference between the voltages produced by the positive and negative impedances. Because this combination of impedances is below threshold over the entire mode spectrum the injection voltages are all of the same sign. This finding has to be contrasted with forced mode locking, where the center portion of the spectrum is above threshold, the wings are below threshold and the equivalent injection locking voltages change sign as one progresses from the center of the line to its edge.

(2.11) may be used to eliminate  $g$ , and from the remaining two equations (2.12) and (1.4) one may obtain two equations for  $P/P_L$  and  $\omega_L \tau_p$  respectively.

$$\frac{1}{g_0} \frac{P}{P_L} = \frac{1/(g_0 \kappa)}{\omega_L \tau_p + \frac{1}{\omega_L \tau_p}} = \left(1 - \frac{1}{g_0}\right) + \frac{1}{\omega_L^2 \tau_p^2} \quad (2.14)$$

Solutions of  $1/\omega_L \tau_p$  vs  $g_0 \kappa$  are shown in Figure 1. It is clear from the figure that under certain conditions no mode locking solutions are found. Indeed, that happens for a fixed excess gain

parameter  $1 - 1/g_0$  when  $g_0\kappa$  becomes too large, i.e. the  $Q$  of the absorber becomes too small or its saturation power  $P_A$  becomes too small. The saturable absorber is too "overpowering", the pulse wants to become too high and too short, and the laser medium cannot adjust itself to it.

An asymptotic expression for  $1/\omega_L\tau_P$  as a function of  $g_0\kappa$  is easily obtained and helps in the interpretation of Figure 2. If one assumes that  $g_0\kappa \ll 1$ , i.e. if one views the portion of the plots closest to the ordinate, and looks for solutions  $1/\omega_L\tau_P \ll 1$ , one may simplify (2.14) to become

$$\frac{1}{\omega_L \tau_P} = \left(1 - \frac{1}{g_0}\right) g_0\kappa \quad (2.15)$$

Thus the lower branches of the curves in Figure 1 are straight lines with slopes proportional to  $\left(1 - \frac{1}{g_0}\right)$ .

Since we have found in general two solutions for each set of parameters corresponding to different pulse widths and intensities one would expect that in general some of these solutions would be unstable. This question will be investigated in another publication. Suffice it to state here that the branch above the "locus of apices" in Figure 1 is found to correspond to unstable solutions, except in the very neighborhood of the locus. There two stable solutions are found within a very narrow regime of  $\kappa g_0$ , for any given  $g_0$ .



### Conclusions:

The problem of a fast saturable absorber has been solved in closed form. The pulse shape is a secant hyperbolic as a function of time. Incidentally, the spectrum has also a secant hyperbolic shape because the secant hyperbolic is its own Fourier transform.

The net gain of the system  $(g - 1)$  is negative before and after the pulse. This is a necessary requirement for the stability of the solution found. Indeed, if the gain had been found positive in the dead-time between the pulses, any disturbance could grow in this time interval and thus destroy the sequence of periodic short pulses. Experimentally observed two photon fluorescence traces produced by picosecond pulses have been compared against assumed gaussian and Lorentzian pulse shapes[1]. The present analysis suggests that the assumption of a hyperbolic secant shape is more plausible.

References

- [1] E. P. Ippen, C. V. Shank, and A. Dienes, "Passive Mode Locking of the cw Dye Laser," Appl. Phys. Lett., vol. 21, no. 8, pp. 348-350, October 1972.

Figure 1.

